Transient Endpoint Perturbations for Identification of Joint Impedance

Experimental Evaluation

K.L. Ragnarsdottir

Master of Science Thesis

TU Delft Delft University of Technology

Biomedical Engineering

Transient Endpoint Perturbations for Identification of Joint Impedance

Experimental Evaluation

Master of Science Thesis

For the degree of Master of Science in Biomedical Engineering at Delft University of Technology

K.L. Ragnarsdottir

November 16, 2014

Faculty of Mechanical, Maritime and Materials Engineering (3mE) · Delft University of Technology

Abstract

To allow for efficient and robust gait pattern, humans instantaneously modulate their joint impedance. Lower-limb amputees and patients suffering from neurological diseases partly lack that ability. Therefore, prosthetic and rehabilitative devices have been designed to restore and repair nominal locomotion. For bio-inspired control of these devices, the underlying physiological behavior of the lower-extremity must be identified and quantified. Deeper understanding is also important to determine appropriate therapy for patients with upper motor neuron diseases. Different identification methods exist to quantify joint impedance during well-controlled, static tasks using continuous random perturbations. However, methods are lacking which quantify joint impedance during walking

The goal of this Master thesis was to experimentally validate a novel method to identify joint impedance during the stance phase of walking. The thesis investigated whether transient endpoint perturbations applied using an instrumented treadmill were sufficient to identify the dynamics of a single-joint system where all properties were known. The influences from the experimental setup were evaluated and finally, the method was applied in a pilot study of a human subject standing on the treadmill.
Results indicate that joint parameters of the system could be consistently estimated with a good fit. However, they were not physically meaningful and did not match the true parameters of the system. This was caused by effects from the experimental setup, which could not be directly subtracted from the data. Model simulation demonstrated the sensitivity of the method to measurement noise.

The limitations of the method and the available experimental setup were carefully identified in this study. Thorough guideline for the method was developed which facilitates the use of the method and sharpens the goal for further research.

Keywords Transient Endpoint Perturbations (TEP), System Identification and Parameter Estimation (SIPE), joint impedance, validation, simulation

Table of Contents

List of Figures

List of Tables

Acknowledgements

I would like to express my sincere gratitude to my supervisors, Dr. -Ing. Heike Vallery and Dipl. -Ing. Anna Pagel, for all their valuable support, assistance and motivation during the course of this master thesis. Furthermore, I would like to thank Dr. Ir. Erwin de Vlugt and Dr. Ir. Jurriaan H. de Groot for all their useful suggestions, critiques and all the valuable work with the setup. Finally, I want to thank my parents and friends for their support and encouragement throughout my studies.

Delft, University of Technology
November 16, 2014

K.L. Ragnarsdottir

Chapter 1

Introduction

1-1 Motivation

Understanding and quantifying the physiological properties of the ankle joint during walking is important to replicate natural gait with active exoprostheses, exoskeletons or orthoses. Only then can the behavior of a healthy ankle be mimicked and used to develop realistic, biologically inspired control schemes for the active devices [3]. Deeper understanding is also clinically relevant for improved diagnosis and therapy assessment of patients suffering from Upper Motor Neuron Disease (UMND)[4].

1-2 Joint impedance

At a first glance, it appears that human walking is a simple, repetitive process that is easily understandable. Learned already at an early age, humans seem to walk with little effort. While interacting with their environment, they can simultaneously alter their walking speed, maintain stability and correct for unexpected disturbances. They can perform a broad spectrum of various movements without paying close attention to how exactly these movements are generated. One means to express the adaption of the joint is the joint impedance. It describes the dynamic relation between the position of the joint and the torque acting about it [3] (Figure 1-1):

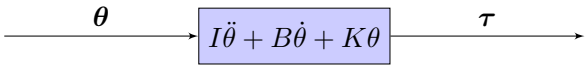

Figure 1-1: Joint impedance: the dynamic relationship between joint angle θ (input) and the resulting torque τ (output) acting about the joint.

Humans show impressive ability to instantaneously modulate their joint impedance during walking [5]. As the heel strikes the ground, the leg muscles must alter their force production

to increase the impedance of the hip, knee and ankle joints. This is essential for carrying the entire body weight, increase stability and to absorb unexpected impact. Insufficient joint impedance might result in stumbling or falling. Simultaneously, the joint impedance of the opposite leg must decrease significantly to ensure that the leg can swing [6].
Two main components have been identified which are responsible for modulating joint impedance during healthy walking. **Intrinsic components** arise from the active and passive properties of the muscles, tissues and tendons around the joint. **Reflexive components** originate as the afferent sensory feedback resulting in the activation of the muscles. Information from the proprioceptors (Muscle Spindles and Golgi Tendon Organs) and the mechanoceptors (sensing pressure, pain and vibrations in the skin) influence the contribution of the reflexive components [7]. To compensate for changes in tasks and environment, each component can be significantly altered and tuned by the Central Nervous System (CNS) [8]. Joint impedance is also known to vary depending on the task [9], the perturbation type [8, 10] and time [11]. To date, it is still under investigation to what extent intrinsic and reflexive components contribute to total impedance.

1-3 State of the art in joint impedance identification

Physiologists and biologists study joint impedance either in *ex vivo* or by experimentally manipulating the physiological behavior of the joint. Some studies use surgical deafferentation while others used vibrations, ischemia or electrical stimulation [12, 13]. The mechanical behavior of the joint under normal condition is then compared to the behavior observed in a joint which has been manipulated. A major challenge is to ensure that conditions are properly matched between the baseline and the manipulated condition. These studies are important to gain fundamental understanding of physiological joint behavior, although results are not verified and are subjective to experimental conditions [14].

The physiological approach is in contrast with the engineering approach, which uses System Identification and Parameter Estimation (SIPE) methods to study joint impedance analytically [8, 10, 15]. SIPE is a discipline that originates from the field of control engineering. It focuses on formulating mathematical models of dynamic systems using measurements of their inputs and outputs. The challenge is to derive a model of the joint dynamic (i.e. the system dynamics) by analyzing the relation between the input (either position or torque) and the output (torque, position or EMG)[16]. The advantages of using SIPE methods is that the internal behavior of the human body can be estimated. The methods are then useful to point out flaws in past theories and to suggest new theories and experiments [17].

Regardless of the system under study, the SIPE process tends to follow the same, logical flow (Figure 1-2). Based on the prior knowledge of the system, an experiment is designed and data is collected. A certain model set is then chosen to describe the system as well as the criterion for the fit. Using the recorded data and the chosen model structure, the parameters of the system's model are calculated. Finally, the calculated model is validated in terms of how well it manages to represent the true dynamics of the system. In case the model is not accurate enough, it must be revised and the whole process is adjusted and repeated [1].

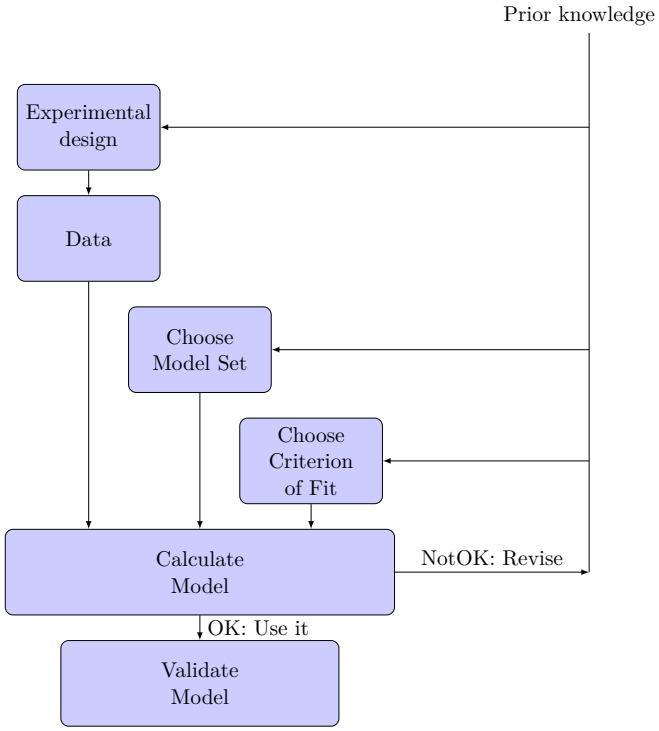

Figure 1-2: The SIPE loop as described in [1]

In the beginning of the identification process, it is important to consider how to describe the dynamics of the joint, i.e. how it should be modeled. The term model refers to the conceptual or quantitative framework which is chosen to describe the system and/or its behavior [16].

Parametric models preferably use a minimal set of parameters to describe a physical system. The models are usually derived from empirical findings or principles which means that *a priori* knowledge is needed about the system. Parametric identification methods are then used to estimate the parameters of the model [14].
Parametric models are useful when the goal is to estimate dynamic behavior but inappropriate without prior knowledge about the system [18]. Parametric identification routines are generally computationally efficient because of their compact representation of the system dynamics. However, in cases where the parametric model differs from the real system, the resulting parameters might be precisely estimated but will not be physically meaningful. Only if the appropriate model structure has been determined can parametric methods be used with confidence [19].

Non-parametric models do not require any *a priori* knowledge about the equations describing the system response. They are useful if a time-varying behavior can be easily repeated [18]. However, the disadvantage is that there is no direct relationship between the estimated non-parametric model and the underlying physiological components responsible for the system's output [20].

Joint impedance experiments generally consist of applying position and/or force perturbations to the joint and measure the resulting joint displacement and torque. Single-joint impedance under static conditions has been thoroughly studied, i.e. by studying only a single joint and keeping the deviations of the joint angle as small as possible. Ankle [9, 21, 22], knee [6, 15], wrist [23] and shoulder [8, 24] have been extensively studied in this manner. Such studies are beneficial to give an insight to the physiological properties of joint impedance, but give limited information about its functional role. Postural studies on both upper [4, 25] and lower [26, 27] extremity are examples of multi-joint studies which have been performed to shed a light on how humans maintain their position and stability.
Existing SIPE methods have also been evaluated and investigated using model simulations [26]. They allow for prediction of the joint behavior under various conditions which might be difficult to implement in reality. They are therefore a meaningful tool to optimize experiments and to reduce the experimental effort.

Compared to the number of dynamic studies on joint impedance, relatively few *in vivo* studies have been done on the human during walking [15]. The challenges of studying the human during walking can partly be explained by the complexity of the human itself. During walking, the human can be viewed as multi-joint system demonstrating both non-linear and time-varying behavior. This behavior is challenging to model using simple linear, time-invarying techniques. The experimental setup poses also limitations. On one hand, the experiment requires a device which applies persistently exciting perturbations to yield useful data which are rich in information [28, 29]. At the same time, the device must not hinder the subject's natural movements [3, 30].

1-4 Problem statement and outline

The properties of the ankle joint during natural, dynamics tasks such as walking have not been determined successfully. Intrinsic ankle joint impedance has been studied by applying transient endpoint perturbation at the sole of the foot [3, 31] during the stance phase of walking. However, the conceptual feasibility of applying such perturbations has never been systematically studied. Furthermore, the influences from the available experimental setup have not yet been evaluated.

The goal of this Master thesis is to experimentally validate a novel identification method, Transient Endpoint Perturbation System Identification and Parameter Estimation (TEP-SIPE). The method was developed to identify ankle joint impedance during the stance phase of walking by applying transient endpoint perturbations using an instrumented treadmill. The recorded data is processed in time-domain by fitting short data segments, including only the perturbation, to a model of the system's dynamics.
The thesis investigates whether the TEP-SIPE method is able to identify the impedance of a single-joint system where all properties are known. The influences from the experimental setup are evaluated and finally, the method is applied in a pilot study of a human subject standing on a treadmill.

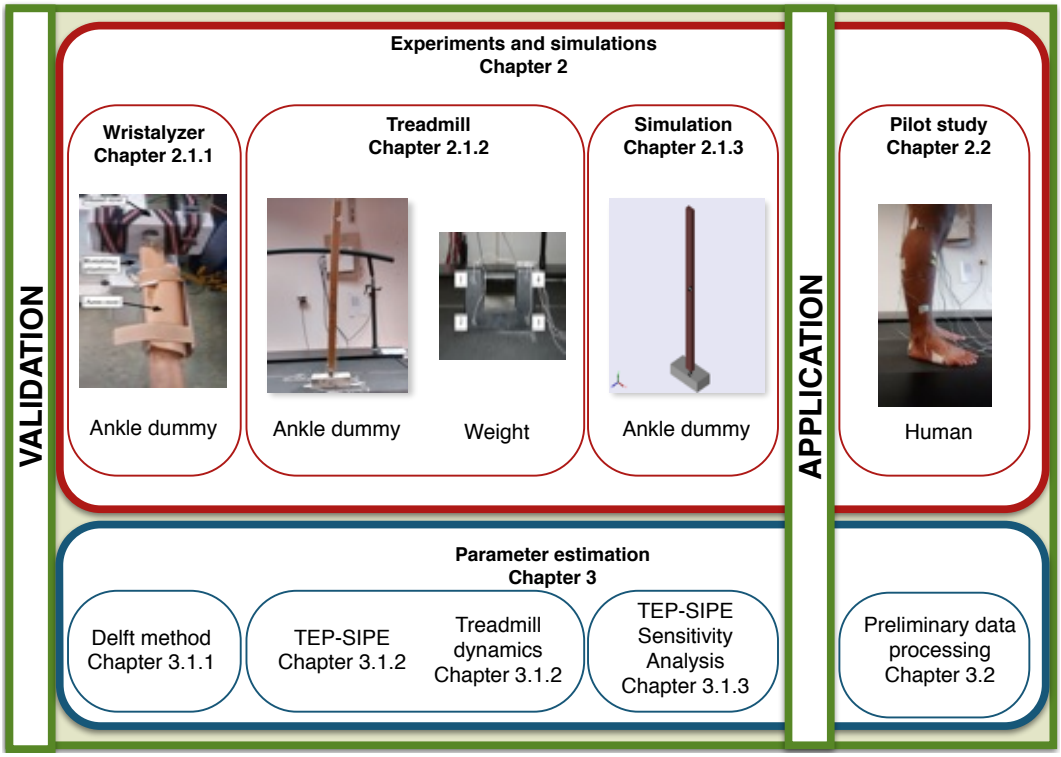

Figure 1-3: Summary of the methods applied in this Master thesis

Chapter 2 addresses the perturbation experiments and simulations conducted to validate the TEP-SIPE method. The true properties of an single-joint ankle dummy were estimated in a benchmark experiment, using the Wristalyzer. The properties of the ankle dummy were then estimated with the TEP-SIPE method, using an instrumented treadmill. Weight experiment was conducted to evaluate the treadmill dynamics. The parameters estimated in the Wristalyzer and on the treadmill were evaluated in a model simulation. The model simulation was also used to investigate the influence of noise on the parameter estimates. As an addition to this study, a pilot study with a human subject standing on a treadmill was performed.

Chapter 3 is concerned with the post processing of the recorded experimental data. The SIPE method to estimate the true parameters of the ankle joint is explained as well as the TEP-SIPE method used for the treadmill data and the model simulation. The evaluation the treadmill dynamics shown as well as the first steps to process the data from the pilot study. For clarity, the outline of chapters 2 and 3 is summarized in Figure 1-3.
Chapter 4 presents the the results from all experiments and model simulations. Preliminary data from the pilot study is shown.
In Chapter 5, the parameters estimated with the TEP-SIPE method are evaluated. The influences from the treadmill dynamics are discussed as well as the results from the model simulation. Outlook is given for future research.
Chapter 6 concludes this study.

Chapter 2

Experiments and simulations

The validation of the TEP-SIPE method was three-fold. First, an established method based on perturbation experiments using the Wristalzyer [32] was used to identify joint impedance of a single-joint ankle dummy. Second, the TEP-SIPE method based on transient endpoint perturbations using an instrumented treadmill [31] was used to identify these parameters. Third, the parameters estimated in the two experiments were evaluated in a model simulation. This was done by simulating the treadmill experiment using a SimMechanics model of the ankle dummy. To define properties of the ankle joint in the simulation, parameters estimated with the Wristalyzer-based SIPE (scenario 1), and with TEP-SIPE (scenario 2) were used. Input to the simulation were the perturbation profiles used in the real treadmill experiment. On the one hand, the resulting movements in both scenarios were compared to the movement recorded from the real treadmill experiments. On the other hand, parameter estimation was conducted using simulated kinematics and torques. The model simulation was also used to investigate the influence of noise on the quality of the parameter estimation. A pilot study was then conducted with a human subject standing on the instrumented treadmill.
The evaluation of the experimental setup was done in a weight experiment. The reliability of recorded forces and moments were investigated to see whether the treadmill dynamics could be successfully determined. Table 2-1 summarizes the experiments and simulations presented in this chapter.

	Validation				**Application**
Setup	Wristalyzer	Treadmill		Simulation	Treadmill
Subject	Ankle Dummy	Ankle dummy	Weight	Ankle dummy	Human
Purpose	Benchmark experiment	TEP-SIPE	Evaluate treadmill dynamics	Evaluate parameter estimates TEP-SIPE Sensitivity analysis	TEP-SIPE

Table 2-1: Overview of experiments and simulations. The method and experimental setup are validated with the ankle dummy and weight. The method is applied on a human in a pilot study

2-1 TEP-SIPE Validation

A simplified model of a leg with a single joint, representing the ankle joint, was needed for the validation. A brick was used as the foot and a wooden rod was used as the leg. The two segments were connected together with a rubber joint representing the ankle joint (Figure 2-1). The geometrical and mechanical properties of the dummy were obtained by directly weighing and measuring the two segments segments (Table 2-2).

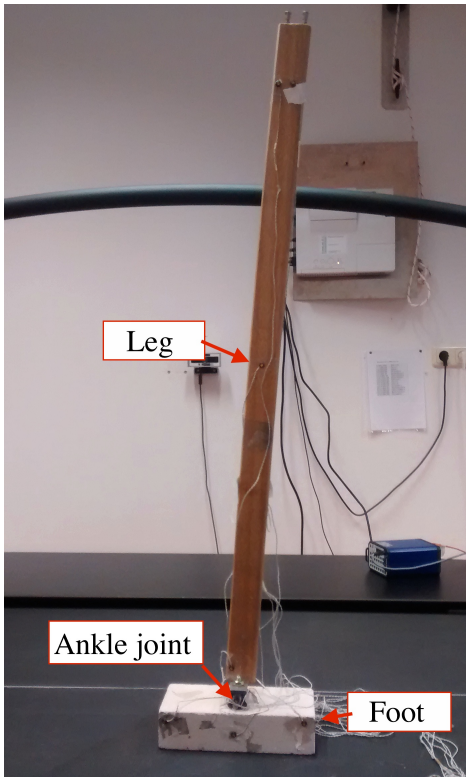

Figure 2-1: The ankle dummy used for the TEP-SIPE validation. The brick, rod and rubber joint represent the foot, leg and ankle joint respectively.

	width [cm]	depth [cm]	length [cm]	mass [kg]	inertia $[kg \cdot m^2]$
Foot	21	10	5.5	2.1	0.008
Leg	4.5	2.5	89.7	0.4	0.027

Table 2-2: Geometrical and mechanical properties of the ankle dummy

2-1-1 Wristalyzer

Experimental setup

The Wristalyzer is a 1 DoF torque-controlled manipulator, intended for dynamic investigation of wrist properties of neurological patients. It can measure the motion of the wrist under various mechanical conditions with a high accuracy [2]. The joint admittance, i.e. the relationship between the applied torque and the resulting position, is assessed by perturbing the joint with torque disturbances and observing the angular deviation [32].

The manipulator is a rotating device which can exert both flexion and extension torques around the joint (Figure 2-2). The drive train is driven by an electromotor attached to the hand and arm rest. A brushless disc motor (Baumüller, DSM130N) drives the manipulator with the motor current supplied by a combined amplifier/control unit (Baumüller BUM60), which includes current feedback to improve motor performance. A SinCos encoder (Stegmann SRS50) is used to accurately measure the joint angle. A torque transducer consisting of strain gauges (HBM, XK13E-3/350) is used to measure the torque exerted by the subject [32].

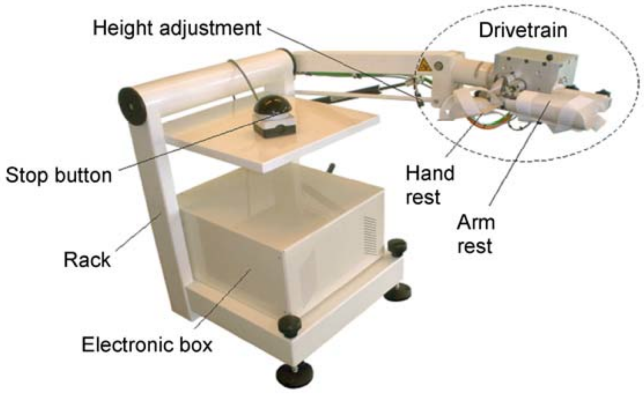

Figure 2-2: The Wristalyzer setup [2]

A control software software application (D-flow, Motek Medical, Amsterdam, Netherlands) was used to apply force perturbations $\tau_P(t)$ to the joint at 2048 Hz. During a single trial, the motor angle $\theta(t)$ was were recorded at approximately 163 Hz.

Experimental protocol

The ankle dummy was fixed to the Wristalyzer (Figure 2-3). The foot was placed on the hand rest and fixed tightly with a strap. The center of the ankle joint was placed directly above the rotating platform of the robot. The leg was fastened to the arm rest using the straps of the setup.

Continuous random force perturbations were applied for 60 sec. The perturbation signal was a multisine signal with a frequency bandwidth ranging from 1 - 20 Hz. Five trials were recorded whith the amplitude of the perturbation signal scaled with five scaling factors: 0.08, 0.12,

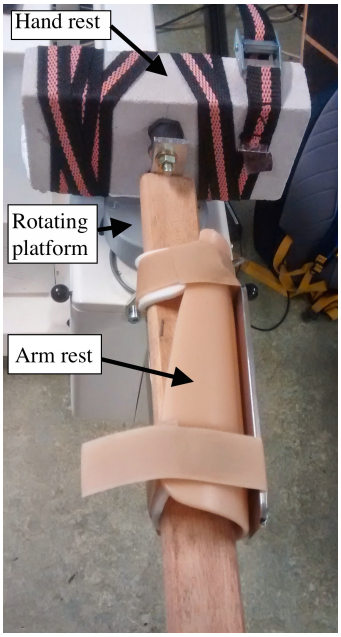

Figure 2-3: Fixation of the ankle dummy in the Wristalyzer. The foot was fixed to the hand rest. The ankle joint was fixed directly above the rotating platform. The rod was fixed tightly to the arm rest.

0.16, 0.20 and 0.24. Signals generated with the lowest scaling factor were just large enough to excite the dynamics of the ankle dummy. Signals generated with the highest scaling factor were just small enough to not damage the dummy. Figure 2-4 shows the perturbation signal, i.e. the torque generated with the lowest and the highest scaling factor.

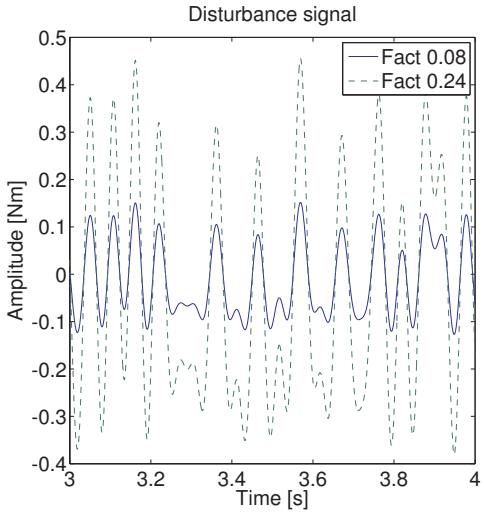

Figure 2-4: Segment of the perturbation signal applied by the Wristalyzer. The solid line shows the signal scaled with the lowest scaling factor (0.08). The dashed line shows the signal when scaled with the highest scaling factor (0.24).

2-1-2 Treadmill

Experimental setup

A dual-belt instrumented treadmill (ForceLink B.V, Culemborg, The Netherlands) measured the forces and moments exerted by the subject. Each belt has 7 force transducers: 4 measure vertical forces, 2 measure medio-lateral forces (ML) and 1 measures anterio-posterior (AP) forces. The transducers are ring torsion load cells with a capacity of 1000 kg (Vishay Revere Transducers, Breda, The Netherlands) and accuracy of ± 0.02%. Using a 12×14 calibration matrix, the 14 signals measured from the two belts were translated to forces and moments referenced to the coordinate system of the treadmill. This resulted in 3 forces (F_x, F_y and F_z) and 3 moments (M_x, M_y and M_z) for each belt. The treadmill belts are actuated at the rear by two ELAU PacDrive high dynamic SM-140 servo motors (Schneider Electric SA, France) with a capacity of 6.5 kW. The treadmill is controlled in real-time using Matlab/Simulink and a xPC Speedgoat target (The Mathworks Inc., Natick, Massachusetts). Belt velocity was generated using voltage signals as input to the treadmill.

The motion was recorded using Optotrak Certus (Northern Digital Inc., Ontario, Canada) motion capture system with a 3D spatial accuracy of ± 0.1 mm. A position sensor detects infrared light emitted by marker diodes and collects the data in reference to a global coordinate system. The markers are activated by a strober controlled by a System Control Unit (SCU). The data from the motion capture system was collected and stored using a software application, First Principles (Northern Digital Inc., Ontario, Canada). To synchronize the motion data to the treadmill data, an external trigger signal was sent from the xPC to the SCU. The data collection, belt movement and perturbations were initialized with a command from the Matlab running on the host computer to the xPC. The forces were sampled at 1000 Hz and motion was sampled at 250 Hz. A schematic of the complete setup is shown in Figure 2-5.

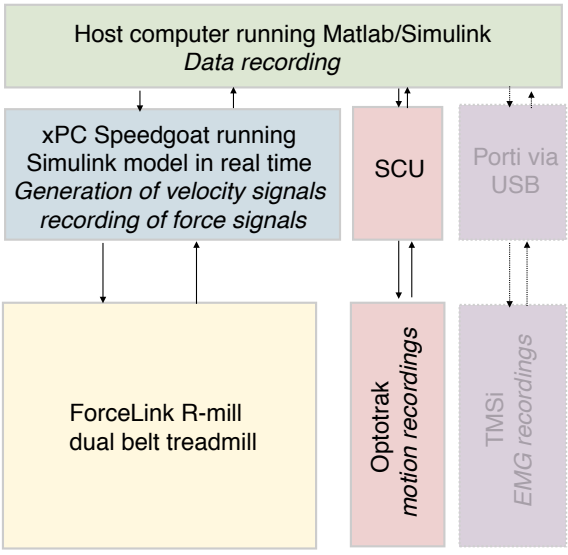

Figure 2-5: Schematic overview of the instrumented treadmill setup. For the ankle dummy and weight experiments, the EMG recordings from the TMSi were not needed.

Experimental protocol

Ankle dummy experiment The ankle dummy was placed on the center of the right belt. Eight active markers were placed on the dummy (Figure 2-6). A double tape under and on the side of the dummy prevented it from from slipping on the treadmill during the experiment. Each trial lasted 70 sec with perturbations applied every 4 sec. One trial was repeated with perturbations applied every 8 sec. This was done to ensure that the effects from previous perturbations had decayed before the next perturbation was applied. The unperturbed position of the dummy was recorded during the first 6 sec and last 8 sec of each trial to obtain the reference position of the dummy.

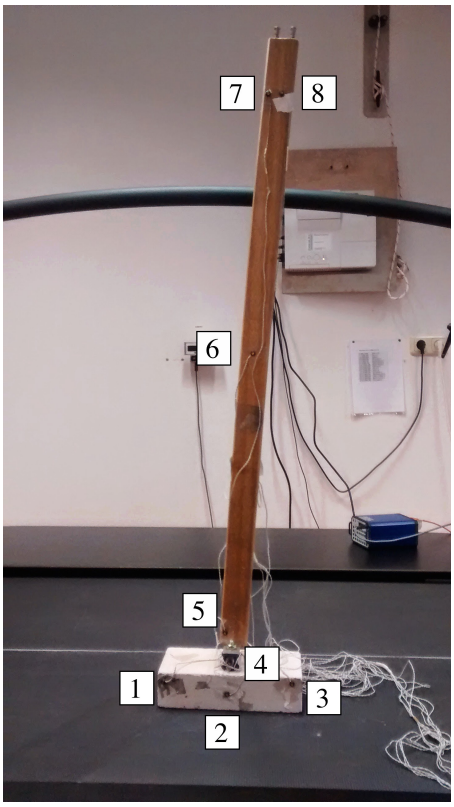

Figure 2-6: The ankle dummy was placed on the right belt of the treadmill. Eight active markers were attached to the dummy: three markers on the foot (markers 1-3), one marker on the ankle joint (marker 4) and four markers on the leg (markers 5-8).

Weight experiment To determine the dynamics of the treadmill, the experiment was repeated when the treadmill was either empty or loaded with a 20 kg weight. The reliability of the treadmill recordings could be evaluated by comparing forces and moments from the empty belt to the forces and moments recorded with a known weight. During loaded trials, the weight was placed in the center of the right belt. Four active markers were placed on the weight (Figure 2-7). A double tape under the weight prevented it from slipping on the treadmill during the experiment. Each trial lasted 60 sec with perturbations applied every

4 sec.

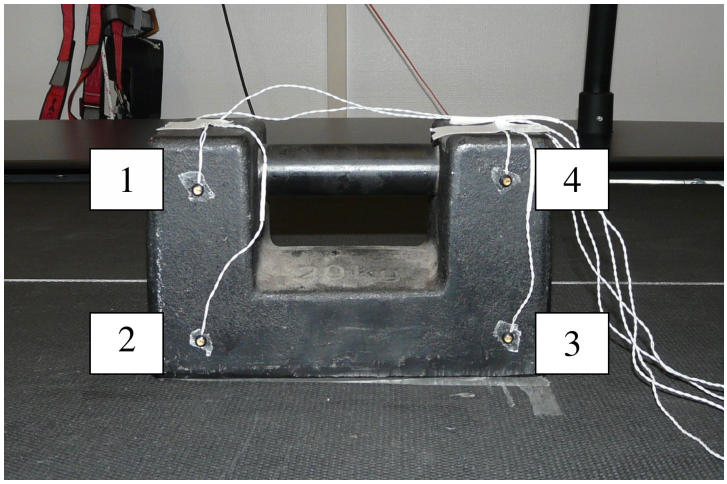

Figure 2-7: The 20 kg weight placed on the treadmill. Four active markers were attached to the dummy, one in each corner.

The same experimental protocol was followed for the ankle dummy, the empty treadmill and the weight (Figure 2-8). The perturbation signal was designed such that it is suitable for human experiments. The perturbation should be strong enough to elicit a reaction in the joint. At the same time it should avoid disturbing the natural gait and should ideally not be noticeable to the subject. Two perturbation profiles were tested: A sinusoidal and a minimum jerk profile (Figure 2-9). The perturbation lasted for 100 ms, which is short compared to the duration of the stance phase, which is around 700-800 ms. Five velocity amplitudes were tested for each perturbation profile, ranging from 0.1 to 0.5 m/s.

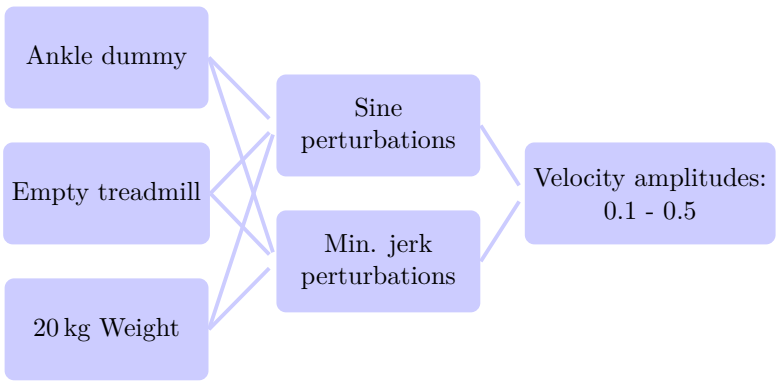

Figure 2-8: The experimental protocol for the ankle dummy, the empty treadmill and the 20 kg weight. Five velocity amplitudes were tested for each perturbation profile. During the ankle dummy experiment, the highest velocity amplitude was applied in two trials. First with perturbation applied every 4 sec and then with perturbations applied every 8 sec. The latter trial was done to ensure that the effects of perturbations had decayed before the next perturbation was applied.

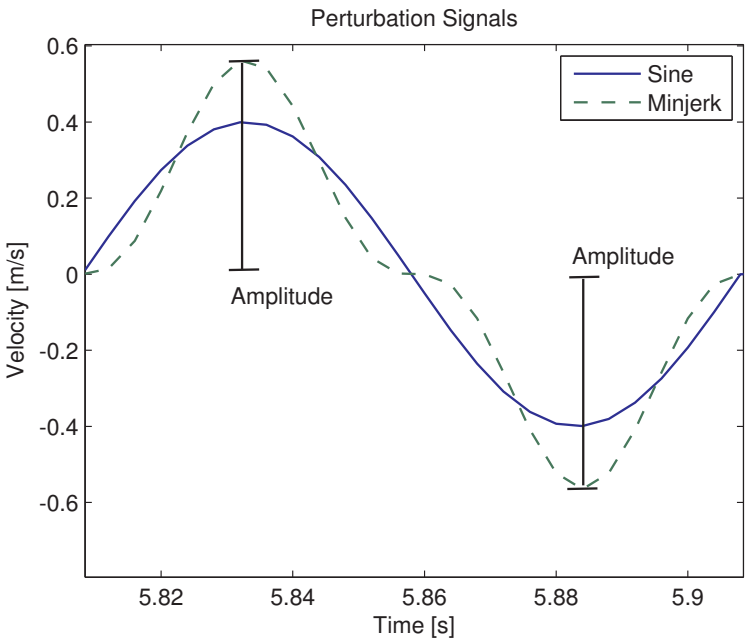

Figure 2-9: An example of the two perturbation signals generated by the treadmill with a sinusoidal velocity of 10 Hz. The velocity amplitude ranged from 0.1 to 0.5 m/s, with the incremental change of 0.1 m/s. The amplitude of minimum jerk profile is indicated in the picture.

2-1-3 Model simulation

Simulation setup

A 3D ankle dummy model was implemented and simulated in Simulink's SimMechanics toolbox (The Mathworks Inc., Natick, Massachusetts) using a fixed step ODE45 solver. To match the sampling rate of the treadmill experiment, the simulation sampling rate was set to 250 Hz. The dummy model was graphically built as blocks representing the foot, ankle joint and the leg (Figure 2-10). The model's geometrical and mechanical properties matched the experimentally measured values of the real dummy. Only 2DoF were modeled: horizontal translation along the y-axis and rotation about the x-axis. The ankle joint was modeled as a second order mass-spring-damper system, which is commonly done to describe the visco-elastic behavior of a mechanical system:

$$\tau_A = I \cdot \ddot{\boldsymbol{\theta}}(t)_A + B \cdot \dot{\boldsymbol{\theta}}(t)_A + K \cdot (\boldsymbol{\theta}(t)_A - \theta_{ref}) \tag{2-1}$$

The parameters I, B, K denote the inertia, damping and stiffness of the ankle joint. The ankle angular position θ_A, velocity $\dot{\theta}_A$ and acceleration $\ddot{\theta}_A$ were measured with a joint sensor. The reference angle θ_{ref} was defined as the resting position of the rod at 0 rad.

Perturbations of the treadmill were realized with a velocity controller. The velocity perturbation profile recorded in the experiment, as well as its derivative and its integration served as input to the controller. Thus, the perturbation caused a horizontal displacement of the foot, identical to the one generated with the treadmill in the real experiment. The ankle joint

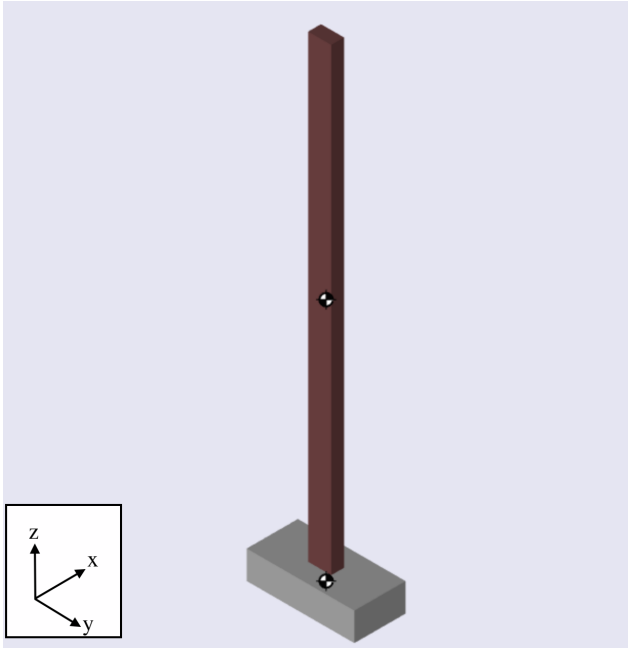

Figure 2-10: The graphical representation of the ankle dummy as visualized in SimMechanics.

torque τ_{Asim}, joint angle θ_{Asim}, velocity $\dot{\theta}_{Asim}$, acceleration $\ddot{\theta}_{Asim}$, ground reaction forces F_{ysim}, F_{zsim}, joint reaction forces F_{Aysim}, F_{Azsim} and the horizontal translation of the foot y_{fsim}, $\dot{y}_{fsim}$, $\ddot{y}_{fsim}$ were recorded.

Simulation protocol

The experimental protocol from the treadmill experiment described in subsection 2-1-2 was repeated twice. First, using I, B and K parameters estimated with the Wristalyzer experiment and second, using I, B and K parameters estimated with the treadmill experiment. The purpose of these simulations was to find out how well the recorded movement of the dummy could be replicated using two sets of parameters. Like that, the correctness of the parameter estimates could be assessed. The validity of the TEP-SIPE method was tested by estimating parameters of the simulated data where parameters were exactly known. Ideally, the TEP-SIPE method should reveal these known parameters.

In a second step, the influence of measurment noise on the parameter estimation was evaluated with a sensitivity analysis. Three configurations of measurement noise were added to the simulated data and evaluated. This was done by adding noise to either the simulated torque, the simulated angular angle or to both torque and angle. For each configuration, the noise level was varied by changing the Signal-to-Noise Ratio (SNR). The SNR is the ratio between the signal power and the noise power. Low SNR indicates that the noise is dominating whereas high SNR indicates that the signal is dominating. The complete simulation protocol is shown in Figure 2-11 and Figure 2-12.

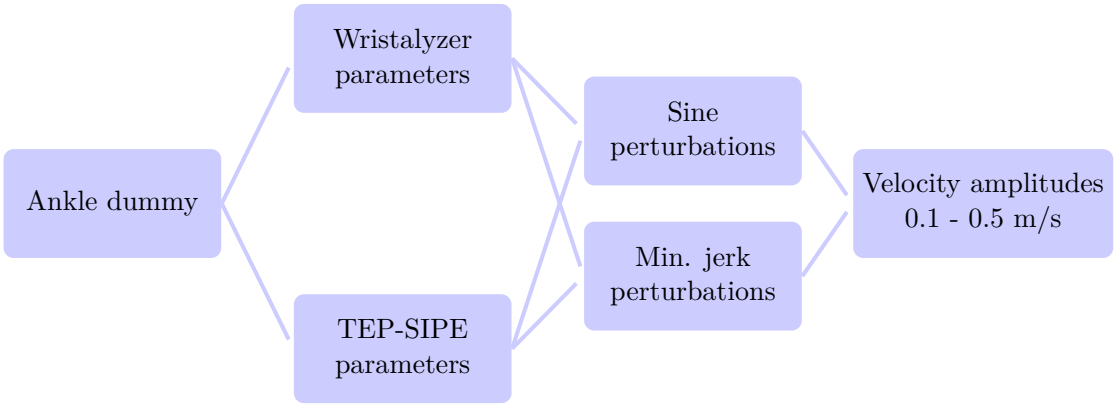

Figure 2-11: The experimental protocol for the first part of the simulation: The parameters estimated with the two different experimental approaches were evaluated in a simulation of the treadmill experiment. The simulated angle torque and angle were compared to the measured torque and angle from the treadmill experiment.

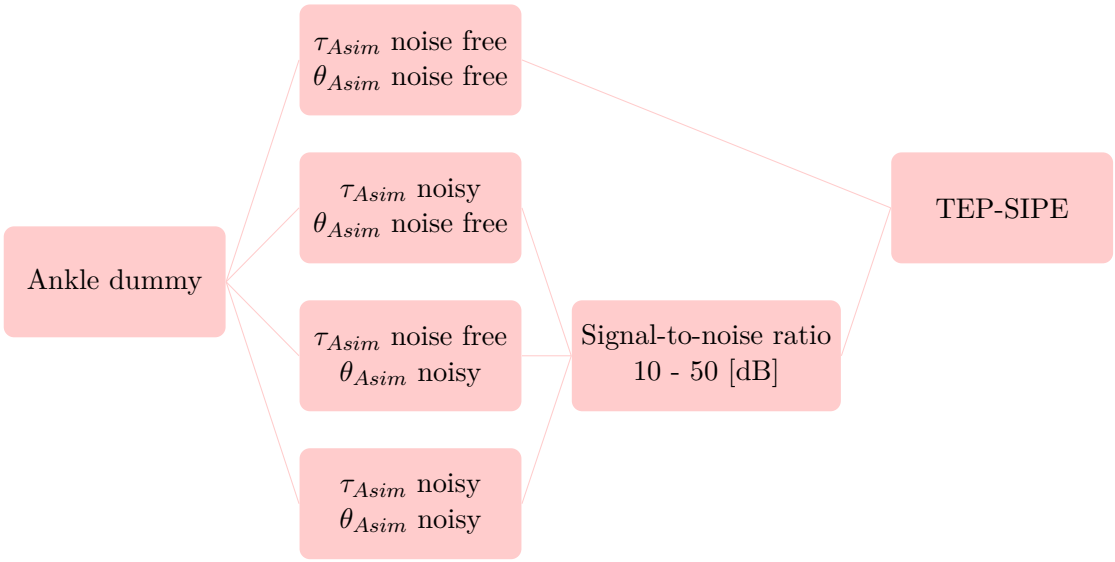

Figure 2-12: The experimental protocol for the second part of the simulation: The ability of the TEP-SIPE method to reveal correct parameters was evaluated by estimating parameters of the simulated datasets. The sensitivity of the method to noise was evaluated by estimating parameters after the simulated data had been corrupted with measurement noise. Noise was added to a) the ankle torque, b) ankle angle and c) both ankle torque and angle.

2-2 TEP-SIPE Application

Experimental setup

A pilot study was performed with one unimpaired female subject (24 years, 175 cm, 64 kg). Eight active markers were placed on the subject; two on the foot, one on the ankle, two at the shank and three at the thigh. Five pairs of electrodes measured the electromyographical (EMG) response of five muscles (Figure 2-13). The signals were recorded with a signal acquisition device (Porti7, TMSi, The Netherlands) at 1000 Hz. A safety harness attached to the ceiling would have caught the subject in the case of falling. The harness did not constrain the subject's movement or provide additional support.

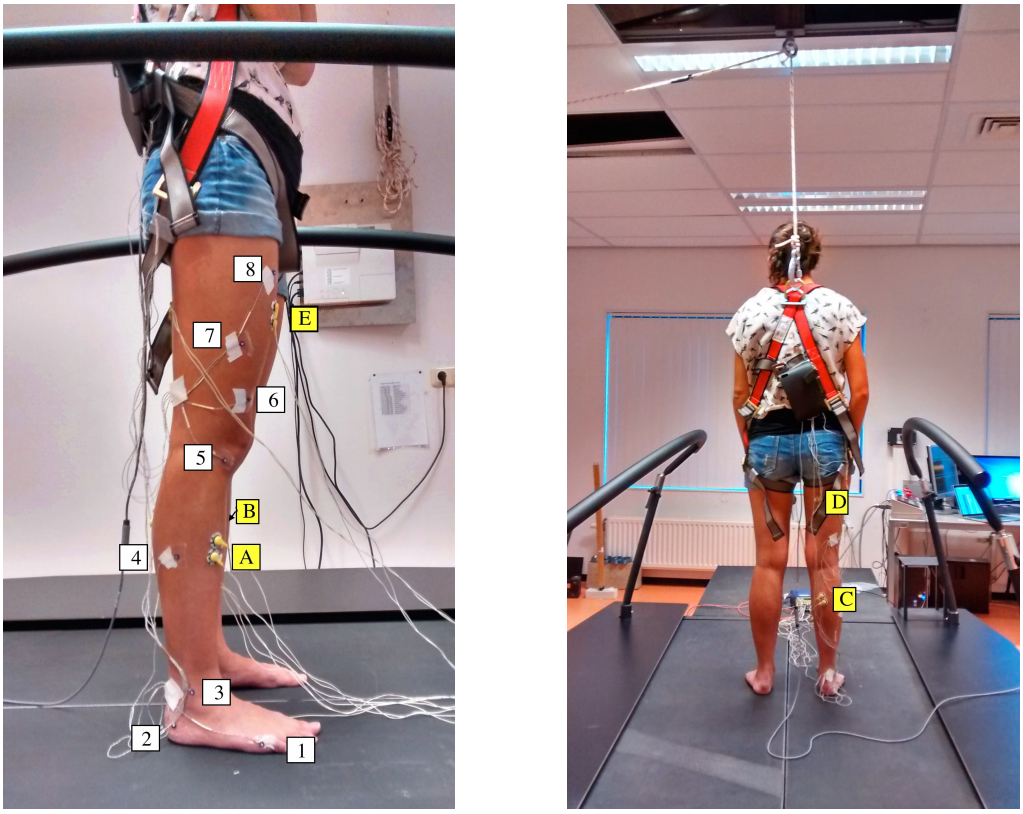

(a) Sagittal view **(b)** Posterior view

Figure 2-13: The placement of the eight motion markers and ten EMG electrodes. The motion markers are labelled from 1-8. The EMG electrodes are labelled from A-E indexing A =Tibialis Anterior (TA), B = Soleus (SOL), C = Gastrocnemius (GAS), D = Biceps Femoris (BF), E = Rectus Femoris (RF).

Experimental protocol

Figure 2-14 shows the experimental protocol, which consisted of 16 trials in total. The subject stood comfortably on the treadmill, placing both feet on the right belt of the treadmill. Two

instructions were giving during the experiment; to relax or to stand as stiff as possible. The subject was asked to keep crossed arms throughout the trial.
Treadmill experiments with the ankle dummy revealed that fit was worse with the minimal jerk profile. Furthermore, the velocity amplitude of 0.1 m/s gave bad fit for both sine and min.jerk perturbation. Those conditions were therefore omitted in the pilot study. Two perturbation profiles, a positive and negative sinusoid, were applied using the treadmill. Four velocity amplitudes were tested for perturbation profile, ranging from 0.2-0.5 m/s. Each trial lasted 65 sec with the perturbations applied randomly every 4-8 sec. The perturbation velocity amplitude was presented randomly between each trial.

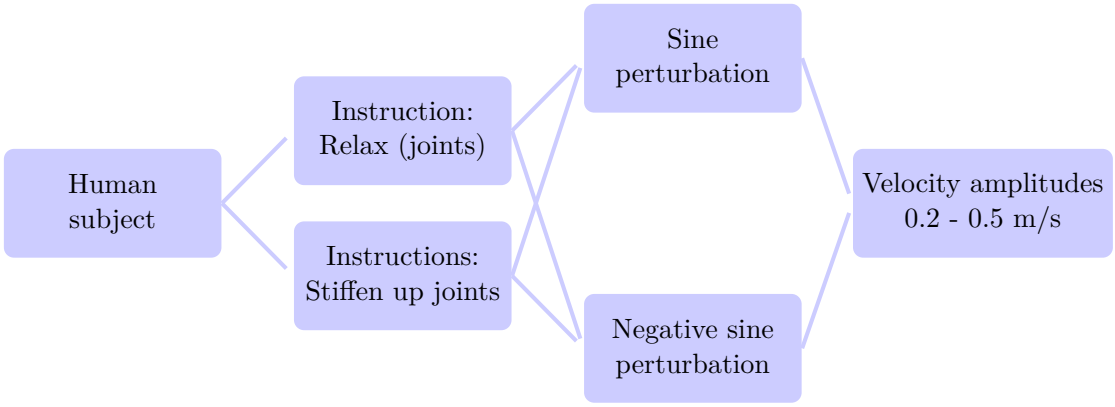

Figure 2-14: The experimental protocol for the pilot study. The subject was given two tasks: to relax or stand as stiff as possible. The two perturbation profiles were tested using velocity amplitudes ranging from 0.2 - 0.5 m/s.

Chapter 3

Parameter Estimation

The true parameters of the ankle dummy were estimated in frequency domain using established identification methods. The TEP-SIPE method was then applied to estimate parameters from the treadmill data and the simulation.
Analyzing and estimating parameters from the pilot study data was not the primary goal of this study. Therefore, data was only post-processed and the parameter estimation is left for future research. As a measure of validity of all parameter estimates, the Variance Accounted For (VAF) was calculated. The VAF gives information about how much of the variance of a signal $\boldsymbol{\theta_A}$ is captured by the predicted signal $\hat{\boldsymbol{\theta}}_{\boldsymbol{A}}$:

$$VAF(\%) = (1 - \frac{\sum_{q(1)}^{q(n)} (\boldsymbol{\theta_A}(t) - \hat{\boldsymbol{\theta}}_{\boldsymbol{A}}(t))^2}{\sum_{q(1)}^{q(n)} \boldsymbol{\theta_A}(t))^2}) \cdot 100\% \tag{3-1}$$

VAF of 100% means that $\hat{\theta}_A$ perfectly describes θ_A [9]. The Standard Error of the Mean (SEM) was calculated to determine how accurately the parameters could be estimated. The accuracy is estimated using the residual error R and the Jacobian J:

$$\boldsymbol{SEM} = \sqrt{\frac{\boldsymbol{R}^T \cdot \boldsymbol{R} \cdot ((\boldsymbol{J}^T \cdot \boldsymbol{J})^{-1})}{\|\boldsymbol{R}\|}} \tag{3-2}$$

Calculating only the VAF for each trial runs the risk of overparameterizing the model. In that case, the model may describe the noise as well as the system dynamics. This is avoided by using a cross-validation prediction. Then, the VAF is computed using a validation dataset different from the reference dataset which is used for the identification. This minimizes the contribution from noise in the estimates and provides a more realistic estimate of the model accuracy [33]. Finally, the treadmill dynamics were evaluated by comparing the data from the empty belt recordings and the weight experiment. All codes for post-processing were customized and specially programmed for this analyzes. Table 3-1 summarizes the post-processing and parameter estimation performed on the experimental and simulated data.

	Validation				**Application**
Experiment	Wristalyzer	Treadmill		Simulation	Pilot study
Subject	Ankle dummy	Ankle dummy	Weight	Ankle dummy	Human
SIPE	TU Delft	TEP-SIPE	–	TEP-SIPE	–
Domain	Frequency	Time			
Recorded Data	τ_P, θ_A	GRF, θ_A	GRF, θ_A	GRF, τ_{Asim}, θ_{Asim}, $\dot{\theta}_{Asim}$, $\ddot{\theta}_{Asim}$	GRF, θ_A, EMG
Filter forces & motion data	4th order bidirectional Butterworth lowpass filter with $f_c = 20$Hz				
Further postprocessing	–	Derive $\dot{\theta}_A$, $\ddot{\theta}_A$ Calculate τ_A from inverse dynamics	Derive $\dot{\theta}_A$, $\ddot{\theta}_A$	–	Derive $\dot{\theta}_A$, $\ddot{\theta}_A$ Calculate τ_A from inverse dynamics Filter EMG
Identification	Admittance $\tau_P(s) \rightarrow \theta_A(s)$	Impedance $\theta_A(t) \rightarrow \tau_A(t)$	Force and mass $\hat{F}_y, \hat{m}_w$	Impedance $\theta_A(t) \rightarrow \tau_A(t)$	– –
Model	$\frac{\theta_A(s)}{\tau_P(s)} = \frac{1}{Is^2 + Bs + K}$	$\tau_A(t) = I\ddot{\theta}_A(t) + B\dot{\theta}_A(t) + K(\theta_A(t) - \theta_{ref})$	–	$\tau_A(t) = I\ddot{\theta}_A(t) + B\dot{\theta}_A(t) + K(\theta_A(t) - \theta_{ref})$	–
Data fitting	Whole dataset	Perturbation only	Whole dataset	Perturbation only	–

Table 3-1: Overview of the various steps taken to post-process the experimental data, to estimate parameters of the ankle dummy and to evaluate the dynamics of the treadmill.

3-1 TEP-SIPE Validation

3-1-1 Wristalyzer

The experimental data was cut and resampled at 256 Hz. It was filtered with a 4^{th} order bidirectional, lowpass Butterworth filter with the cutoff frequency of 20 Hz. The first and last 6 sec were cut off to remove the transients parts of the data.

Non-parametric fitting

The admittance of the joint was estimated non-parametrically in frequency domain by calculating the open-loop spectral estimate $\hat{H}_{\tau\theta}(f)$:

$$\hat{H}_{\tau\theta}(f) = \frac{\hat{S}_{\tau\theta}(f)}{\hat{S}_{\tau\tau}(f)} \tag{3-3}$$

in which $\hat{S}_{\tau\theta}(f)$ denotes the cross-spectral density of external torque perturbation $\tau_p(f)$ and the ankle joint angle $\theta_A(f)$. $\hat{S}_{\tau\tau}(f)$ denotes the auto-spectral density of the external torque perturbation. To reduce the variance, the data was frequency averaged before calculating the cross- and auto-spectral densities. The linearity of the model was checked with the coherence:

$$\hat{\Gamma}_{\tau\theta}(f) = \frac{\mid \hat{S}_{\tau\theta}(f) \mid^2}{\hat{S}_{\tau\tau}(f) \cdot \hat{S}_{\theta\theta}(f)} \tag{3-4}$$

The coherence function $\hat{\Gamma}_{\tau\theta}(f)$ ranges from 0 to 1. Low coherence indicates no linearity while 1 indicates a linear system without noise.

Parametric fitting

The admittance was estimated parametrically by fitting the spectral estimate $\hat{H}_{\tau\theta}(f)$ to a second order linear mass-spring-damper model:

$$\hat{H}_{model}(s) = \frac{\theta_A(s)}{\tau_P(s)} = \frac{1}{Is^2 + Bs + K} \tag{3-5}$$

Hereby, $s = \lambda + \jmath 2f$ with $\lambda = 0$, the admittance of the joint is described wit inertia I, damping B and stiffness K components. A non-linear least-squares algorithm was used for the parameter estimation. The open loop spectral estimate $\hat{H}_{\tau\theta}(f)$ showed that the system's dynamics were dominating on frequencies below 9 Hz (Figure 3-1). Parameters were therefore estimated on the frequency range of 1-9 Hz. Fitting the model to higher frequency would include noise or the effects of the straps used to fasten the foot to the hand rest. The fit procedure was guided with boundaries to prevent negative parameter values and bad convergence (Table 3-2). The fit criterion was chosen as the squared logarithmic difference between the nonparametric model $\hat{H}_{\tau\theta}(f)$ and the parametric model $\hat{H}_{model}(f)$ according to eq: (3-6). The logarithmic difference was multiplied with $\sqrt{\frac{1}{f_{vec}}} \cdot \Gamma_{\tau\theta}(f)$ to compensate for few data in low frequency regions and to emphasise reliable frequencies:

$$e = \sqrt{\frac{1}{f_{vec}}} \cdot \Gamma_{\tau\theta}(f) \cdot \mid \log \frac{\hat{H}_{\tau\theta}(f)}{\hat{H}_{model}(f)} \mid \tag{3-6}$$

A schematic overview of the steps taken during the post-processing is found in Appendix A.

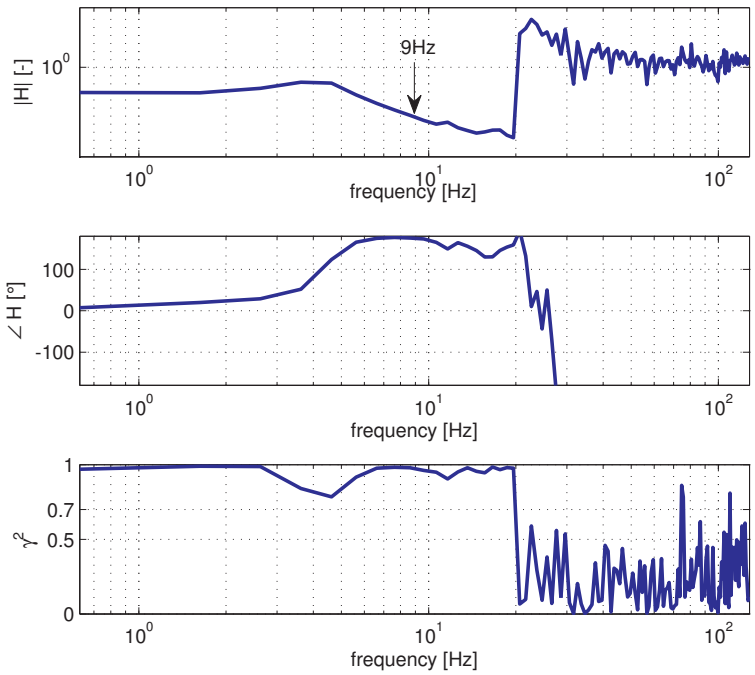

Figure 3-1: Top: The spectral estimate, $\hat{H}_{\tau\theta}(f)$, shows that the ankle dummy is not excited at frequencies higher than 9 Hz. This determined the choice of frequency band estimation. Center: The phase. Bottom: The coherence drops significantly for frequencies higher than 20 Hz.

	I	B	K
Initial search values	0.001	0.1	10
Lower boundaries	-10	0.01	-20
Upper boundaries	10	10	20

Table 3-2: Initial values and parameter boundaries guiding the fit procedure.

3-1-2 Treadmill

Ankle dummy The force and marker data was cut and re-sampled at 250 Hz. A 4^{th} order, bidirectional lowpass Butterworth filter with cutoff frequency of 20 Hz was used to filter the data. The marker data provided the segment coordinates of the CoM (CoM) (foot: y_f, z_f, leg: y_{leg}, z_{leg}). The segment angles θ_f and θ_{leg} and joint angle θ_A were derived from marker data using standard rigid body approach. The angles were defined w.r.t. the vertical axis. Velocities and accelerations were obtained by taking the first and second derivative of the position and angle (foot: $\dot{y}_f$, $\ddot{y}_f$, $\dot{\theta}_f$, $\ddot{\theta}_f$, leg: $\dot{y}_{leg}$, $\ddot{y}_{leg}$, $\dot{\theta}_{leg}$, $\ddot{\theta}_{leg}$, ankle joint: $\dot{\theta}_A$, $\ddot{\theta}_A$).
The sum of forces and moments acting about the two segments (foot: $\sum F_{fy}$, $\sum F_{fz}$, $\sum M_f$, leg: $\sum F_{legy}$, $\sum F_{legz}$, $\sum M_{leg}$) are described with the equations of motion (3-7). The geometrical and mechanical properties l_f, l_{leg}, m_f, m_{leg}, I_f and I_{leg} were presented in Table 2-2. The forces F_y and F_z denote the ground reaction forces measured with the treadmill (Figure 3-2).

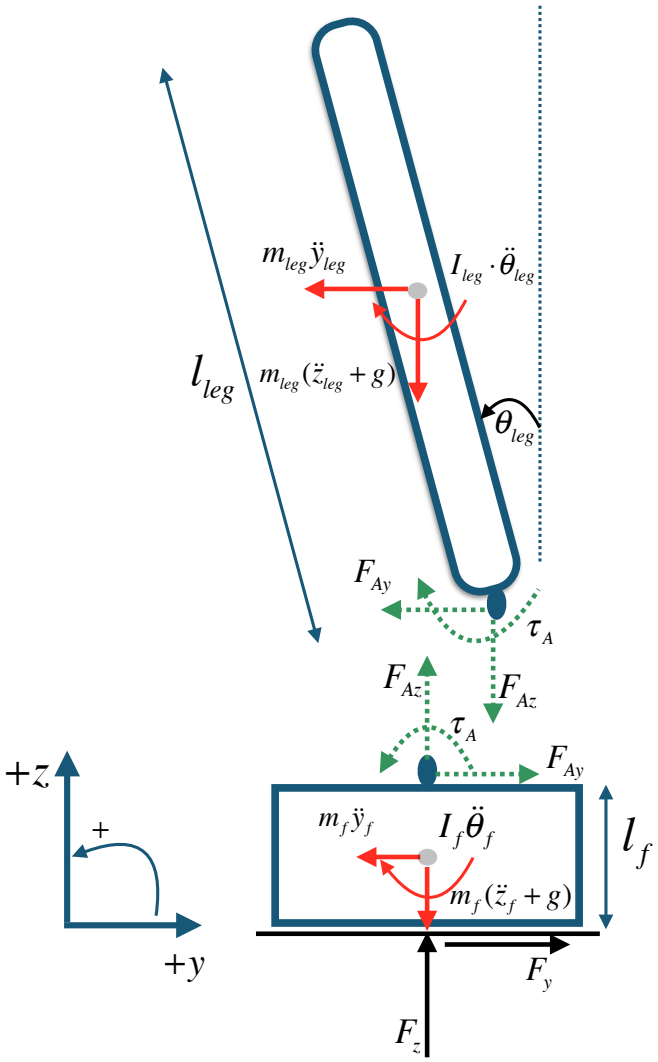

Figure 3-2: Two dimensional free body diagram of the ankle dummy. The unknown joint reaction forces F_{Ay}, F_{Az} and ankle torque τ_A are denoted with dotted, green lines.

$$
\begin{aligned}
\sum F_{fy} &= F_y + F_{Ay} - m_f \cdot \ddot{y}_f = 0 \\
\sum F_{fz} &= F_z + F_{Az} - m_f \cdot g - m_f \cdot \ddot{z}_f = 0 \\
\sum M_f &= F_y \cdot \frac{l_f}{2} - F_{Ay} \cdot \frac{l_f}{2} + \tau_A - I_f \cdot \ddot{\theta}_f = 0 \\
\sum F_{legy} &= -F_{Ay} - m_{leg} \cdot \ddot{y}_{leg} = 0 \\
\sum F_{legz} &= -F_{Az} - m_{leg} \cdot g - m_{leg} \cdot \ddot{z}_{leg} = 0 \\
\sum M_{leg} &= -F_{Ay} \cdot \frac{l_{leg}\cos(\theta_{leg})}{2} - F_{Az} \cdot \frac{l_{leg}\sin(\theta_{leg})}{2} - \tau_A - I_{leg} \cdot \ddot{\theta}_{leg} = 0
\end{aligned}
\tag{3-7}
$$

These six equations are sufficient to calculate the unknown ankle joint forces F_{Ay} and F_{Az} and the ankle joint torque τ_A:

$$\begin{aligned} F_{Ay} &= -m_{leg} \cdot \ddot{y}_{leg} \\ F_{Az} &= -m_{leg} \cdot g + m_{leg} \cdot \ddot{z}_{leg} \\ \tau_A &= -F_{Ay} \cdot \frac{l_{leg}\cos(\theta_{leg})}{2} - F_{Az} \cdot \frac{l_{leg}\sin(\theta_{leg})}{2} - I_{leg} \cdot \ddot{\theta}_{leg} \end{aligned} \tag{3-8}$$

Parametric fitting

The ankle dummy parameters were estimated in time-domain. The data was segmented into short windows including only the length of the perturbation. It was noted that the actual perturbation signal applied by the treadmill was longer then the 100 ms signal command sent from the host computer. Therefore, the size of the evaluation window was adjusted to include the the actual length of the perturbation (Figure 3-3). Each data segment served as input to solve the linear equation describing the properties of the ankle joint:

$$\boldsymbol{\tau_A}(t) = I \cdot \ddot{\boldsymbol{\theta}}_{\boldsymbol{A}}(\boldsymbol{t}) + B \cdot \dot{\boldsymbol{\theta}}_{\boldsymbol{A}}(t) + K \cdot (\boldsymbol{\theta_A}(t) - \theta_{ref}) \tag{3-9}$$

The mean I,B,K parameters from all data segments were used to predict the ankle torque

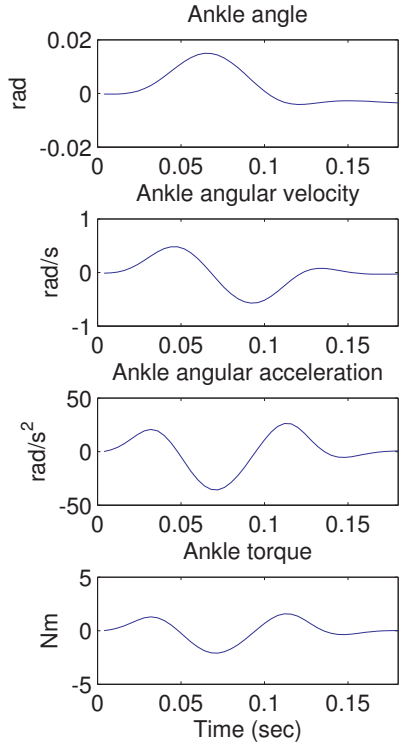

Figure 3-3: An example of the window segment used for the parametric fitting. The example data is from a sinusoidal perturbation with the velocity amplitude of 0.5 m/s.

of the whole dataset. The VAF (eq. 3-1) and SEM (eq. 3-2) values were calculated to evaluate the quality of the fit, both for each single perturbation and for the complete dataset. Furthermore, the mean set of parameters from every trial was used as a reference data for a cross-validation. A full schematic overview of all the steps for the post-processing and parameter estimation is found in Appendix A.

Weight experiment The data was segmented into short windows of 300 ms, starting with the perturbation onset. The ideal force $\hat{\boldsymbol{F}}_{\boldsymbol{y}}$ that should theoretically be measured during the weight experiment was calculated from accelerations:

$$\hat{\boldsymbol{F}}_{\boldsymbol{y}} = m_w \cdot \ddot{\boldsymbol{y}}_{\boldsymbol{w}} \tag{3-10}$$

The ideal force $\hat{\boldsymbol{F}}_{\boldsymbol{y}}$ was then subtracted from the actual force $\boldsymbol{F}_{\boldsymbol{y}}$ measured with the treadmill. The difference between the ideal and measured force was then compared to the force $\boldsymbol{F}_{\boldsymbol{y0}}$ measured with an empty belt. Ideally, the difference between the ideal and measured force during the weight experiment should only arise from the treadmill dynamics so that:

$$\hat{\boldsymbol{F}}_{\boldsymbol{y}} - \boldsymbol{F}_{\boldsymbol{y}} = \boldsymbol{F}_{\boldsymbol{y0}} \tag{3-11}$$

If that was the case, it should be sufficient to subtract the forces $\boldsymbol{F}_{\boldsymbol{y0}}$ from the experimental data to remove the effects of treadmill dynamics. To evaluate reliability of recorded forces, the known mass of the weight was compared to the mass solved from the linear equation:

$$\hat{m}_w = \ddot{\boldsymbol{y}}_{\boldsymbol{w}} \backslash \boldsymbol{F}_{\boldsymbol{y}} \tag{3-12}$$

3-1-3 Model simulation

To avoid biased results when using τ_{Asim} directly from a joint sensor, the ankle torque was calculated with inverse dynamics as $\tau_{Asim} = -F_{ysim} \cdot \frac{l_f}{2} + F_{Aysim} \cdot \frac{l_f}{2} + I_f \cdot \ddot{\theta}_f$. Since the foot was not allowed to rotate, $\ddot{\theta}_f = 0$. After the measurement noise had been added to the simulated data, it was filtered with a 4^{th} order, bidirectional lowpass Butterworth filter with cutoff frequency of 20 Hz. This was done to be consistent with the post-processing of the treadmill data.

Parametric fitting

The force and marker data was cut and re-sampled at 250 Hz. The data was then segmented to short windows containing only the perturbations. The parametric fitting and validation was then performed in the same manner as explained for the treadmill experiment using eq: (3-9).

3-2 TEP-SIPE Application

The post-processing and calculation of segment and joint angles was done in similar fashion as with the ankle dummy data. The Center of Pressure (CoP) of the foot was calculated as:

$$y_{CoP} = \frac{M_x}{F_z} \tag{3-13}$$

where the M_x and donates the moment around the x-axis as measured with the treadmill.

The EMG data was processed according to standard guidelines provided by SENIAM [1]. First, the EMG signals were filtered with a 4^{th} order bidirectional Butterworth filter with the frequency bandwith of 20-300 Hz. The signals were then rectified by taking their absolute value. Finally, the the data was lowpass filtered with a 4^{th} order bidirectional Butterworth filter with a cutoff frequency of 6 Hz. The use of a bidirectional filter for the EMG data was chosen to be consistent with the filtering of the force and motion data.

The ankle torque was calculated by summing the moments around the ankle joint, applying the parallel axis theorem on the moment of inertia and solving for τ_A:

$$\begin{aligned}\boldsymbol{\tau_A} = (\boldsymbol{y_A} - \boldsymbol{y_{CoP}}) \times \boldsymbol{F_y} - (\boldsymbol{y_A} - \boldsymbol{y_f}) \times (m_f \cdot \boldsymbol{\ddot{y}_f}) \\ - (\boldsymbol{y_A} - \boldsymbol{y_f}) \times (m_f \cdot g) - I_f + m_f \cdot \boldsymbol{r_{Af}}\end{aligned} \tag{3-14}$$

y_A and y_f denotes the y-position of the ankle joint and the CoM of the foot, respectively. $\ddot{y}_A$ is the acceleration of the CoM of the foot. r_{Af} denotes the distance between the ankle joint and the CoM of the foot.
The segmentation of the data and fitting it to a parametric model was not part of this study.

[1] www.seniam.org

Chapter 4

Results

4-1 TEP-SIPE Validation

4-1-1 Wristalyzer

The parametric model estimate $\hat{H}_{model}(f)$ was able to represent the nonparametric spectral estimate $\hat{H}_{\tau\theta}(f)$. Coherence was high on all frequencies but dropped down to 0.737 around the eigenfrequency of 4.6 Hz (Figure 4-1).

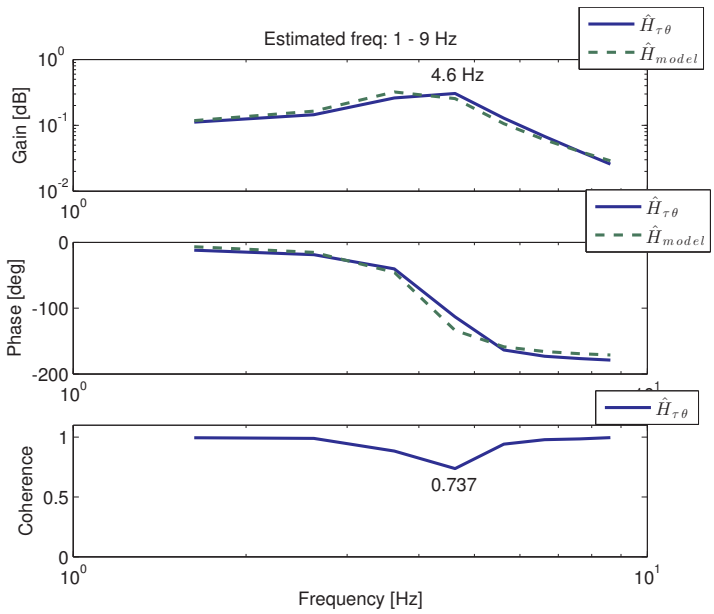

Figure 4-1: The spectral estimate (solid line) compared to the model prediction (dashed line) when the perturbation signal was scaled by a factor of 0.16.

The I B, K parameters could be consistently estimated for all scaling factors (Table 4-1). Validation with the same dataset gave high VAFs for all scaling factors, ranging from 87-95% (Figure 4-2). Cross-validation with different datasets gave also high VAFs, with the mean values from each reference dataset ranging from 84-94% (Figure 4-3). The inertia and damping parameters could be accurately estimated as can be seen by low SEM values. The stiffness was estimated less accurately as can be seen by higher SEM values.

	Dfact 0.08	Dfact 0.12	Dfact 0.16	Dfact 0.20	Dfact 0.24
I [Nms^2/rad]	0.015	0.015	0.015	0.015	0.015
B [Nms/rad]	0.099	0.101	0.097	0.101	0.101
K [Nm/rad]	10.012	10.000	9.967	10.000	10.000
SEM of I [-]	0.021	0.026	0.019	0.014	0.013
SEM of B [-]	0.180	0.177	0.130	0.123	0.126
SEM of K [-]	13.793	17.021	12.260	8.521	7.510
error [-]	1.268	1.304	1.472	1.788	1.952
VAF [%]	91	94	**95**	91	87
$\overline{VAF}_{C-V}$[%]	88	92	**94**	90	84

Table 4-1: The estimated parameters from the Wristalyzer. The best fit was found for Dfact = 0.16. Validation with the same dataset and cross-validation (C-V) with other datasets resulted in high VAFs for all set of parameters.

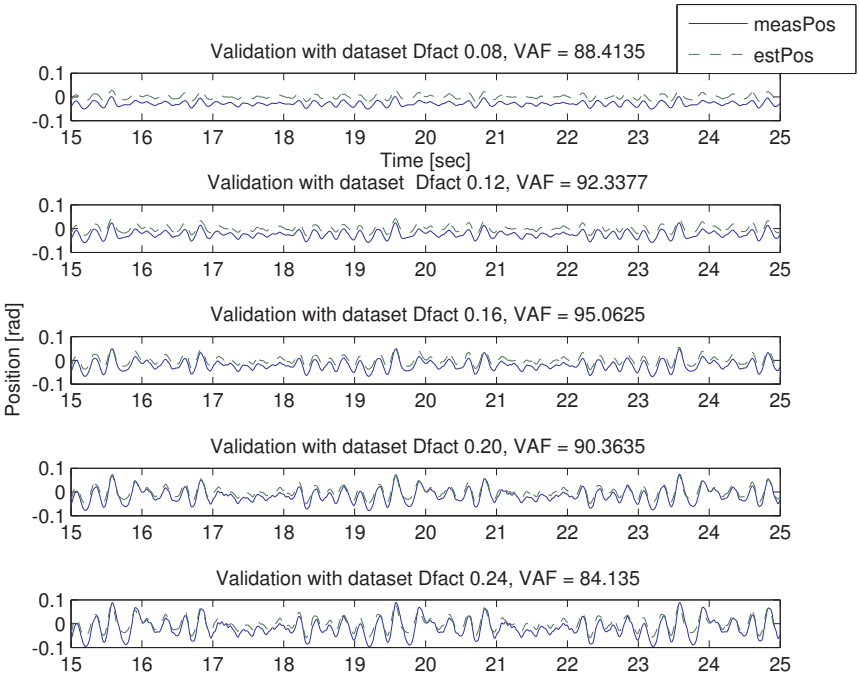

Figure 4-2: Prediction in time domain using the parameters estimated from a dataset with scaling factor Dfact = 0.16. The VAF ranged from 84 - 95 %. For a better observation, only ten seconds of data are presented.

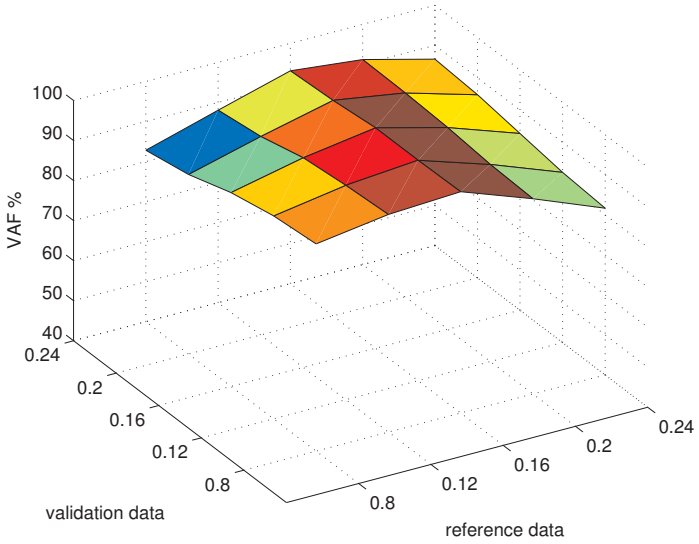

Figure 4-3: Surface plot of the cross validation. The mean VAF values range from 81 - 95% for all datasets.

4-1-2 Treadmill

The TEP-SIPE method could estimate parameters with high VAFs and low SEM values. This was true for both sinusoidal and mininum jerk perturbation profiles. (Table 4-2 and 4-3). Increasing the perturbation velocity amplitude lowered the standard deviation of the parameter estimates (Figure 4-4). Cross-validation gave high VAF values ($> 99,5\%$) for all datasets.

	Sinusoidal perturbation profile					
	Velocity Amplitude [m/s]					
	0.1	0.2	0.3	0.4	0.5	0.5_2
I [Nms^2/rad]	0.061	0.061	0.614	0.061	0.061	0.061
B [Nms/rad]	-0.007	-0.008	-0.006	-0.002	-0.002	0.0138
K [Nm/rad]	6.722	6.629	6.913	5.499	5.341	4.533
SEM of I [-]	$2{\cdot}10^{-4}$	$8{\cdot}10^{-4}$	$1.6\cdot10^{-4}$	$8.7\cdot10^{-5}$	$1.3{\cdot}10^{-4}$	$1{\cdot}10^{-4}$
SEM of B [-]	0.009	0.003	0.006	0.004	0.006	0.005
SEM of K [-]	0.470	0.199	0.322	0.219	0.342	0.246
$\overline{VAF}$ of perturbation [%]	99.99	99.99	99.99	99.99	99.98	99.99
VAF of full dataset [%]	99.8	99.93	99.92	99.92	99.93	99.94

Table 4-2: The parameters estimated with the TEP-SIPE method as well as their SEM and VAF values. Sinusoidal perturbations were applied with the velocity amplitude ranging from 0.1 - 0.5 m/s. The velocity amplitude denoted as 0.5_2 indicates the trial where perturbations were applied every 8 sec instead of every 4 sec.

	Minimum Jerk perturbation profile					
	Velocity Amplitude [m/s]					
	0.1	0.2	0.3	0.4	0.5	0.5_2
I [Nms^2/rad]	0.061	0.061	0.611	0.061	0.061	0.061
B [Nms/rad]	-0.011	-0.009	-0.008	-0.002	0.010	0.009
K [Nm/rad]	6.611	6.104	5.849	5.579	4.798	4.709
SEM of I [-]	$2.7{\cdot}10^{-4}$	$1.7{\cdot}10^{-4}$	$1\cdot10^{-4}$	$2\cdot10^{-4}$	$8\cdot10^{-5}$	$8{\cdot}10^{-5}$
SEM of B [-]	0.013	0.008	0.005	0.006	0.004	0.004
SEM of K [-]	0.700	0.445	0.284	0.330	0.219	0.227
$\overline{VAF}$ of perturbation [%]	99.94	99.98	99.99	99.99	99.99	99.99
VAF of full dataset [%]	99.49	99.88	99.94	99.95	99.94	99.92

Table 4-3: The parameters estimated with the TEP-SIPE method as well as their SEM and VAF values. Mininum jerk perturbations were applied with the velocity amplitude ranging from 0.1 - 0.5 m/s. The velocity amplitude denoted as 0.5_2 indicates the trial where perturbations were applied every 8 sec instead of every 4 sec.

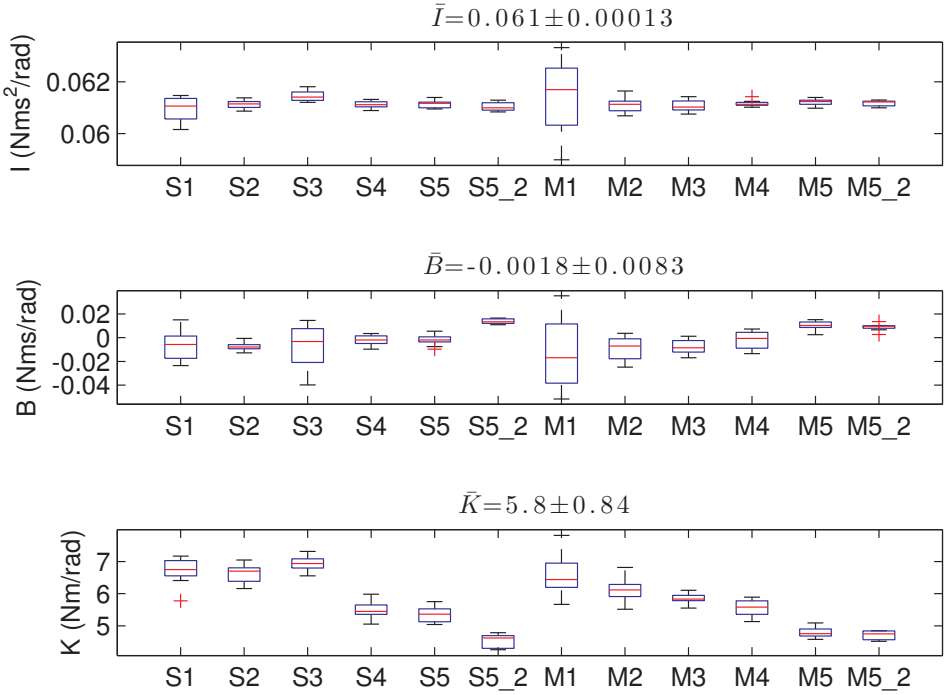

Figure 4-4: Box plot of the parameters estimates with the TEP-SIPE method over all perturbation profiles. The labels S and M denote sinusoidal and mininum jerk profiles, respectively. The numbers 1-5 denote the perturbation velocity amplitude ranging from 0.1-0.5 m/s, respectively. The labels S52 and M52 denote the trial where perturbations were applied every 8 sec instead of 4 sec. $\overline{I}$, $\overline{B}$, $\overline{K}$ denote the mean of parameter estimates over all datasets.

Weight Experiment The mean forces F_{y0} recorded with the empty belt did not match the difference ΔF_y between the actual and ideal forces F_y and $\hat{F}_y$ (Figure 4-5). ΔF_y was highest in turning points of the treadmill, i.e. during maximum velocity. The difference increased as the perturbation amplitude increased and was highest for the mininum jerk profile with amplitude of 0.5 m/s. The standard deviation of the estimated mass $\hat{m}_w$ was highest for low velocity amplitudes (sine 0.1 m/s = 20.±0.5 kg and min.jerk 0.1 m/s = 19.7±0.9kg). As the perturbation amplitude increased, the mass estimation decreased (sine 0.5 m/s = 19.5±0.2 kg and min.jerk 0.5 m/s = 19.4±0.2 kg) (Figure 4-6).

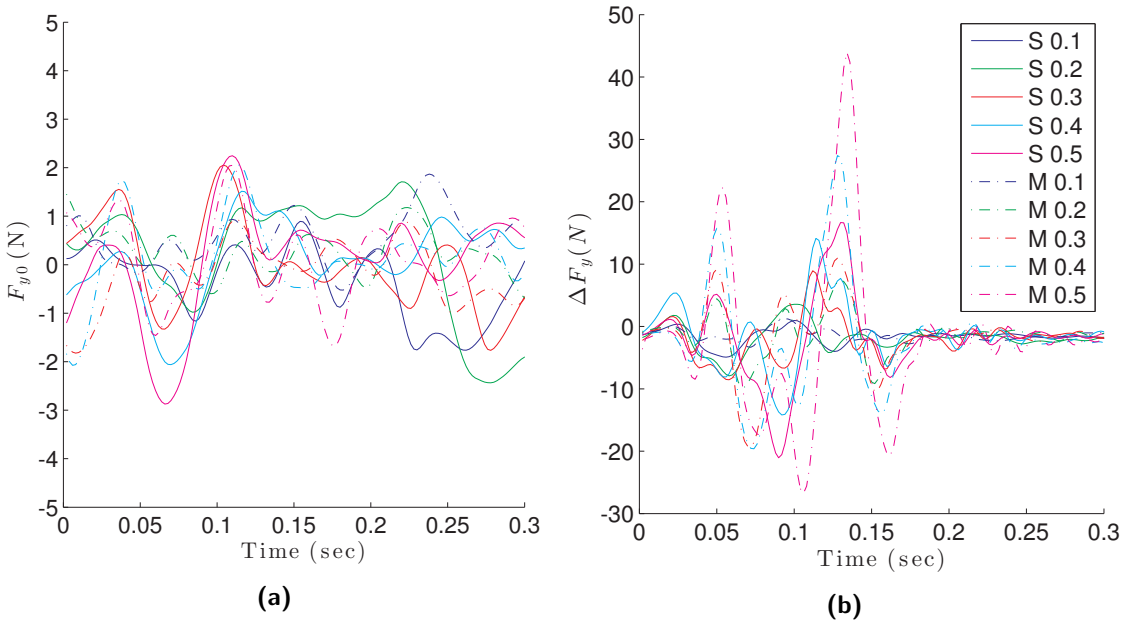

Figure 4-5: a) The mean of forces F_{y0} over all perturbations recorded from the empty treadmill. b) The mean of $\Delta F_y = \hat{F}_y - F_y$ over all perturbations recorded in the weight experiment. The legends S0.1 - S0.5 denote sinusoidal perturbations with velocity amplitudes ranging from 0.1-0.5 m/s. The legends M0.1 - M0.5 denote minimum jerk perturbations with velocity amplitudes ranging from 0.1-0.5 m/s. Note, that the scaling of the y-axis is different.

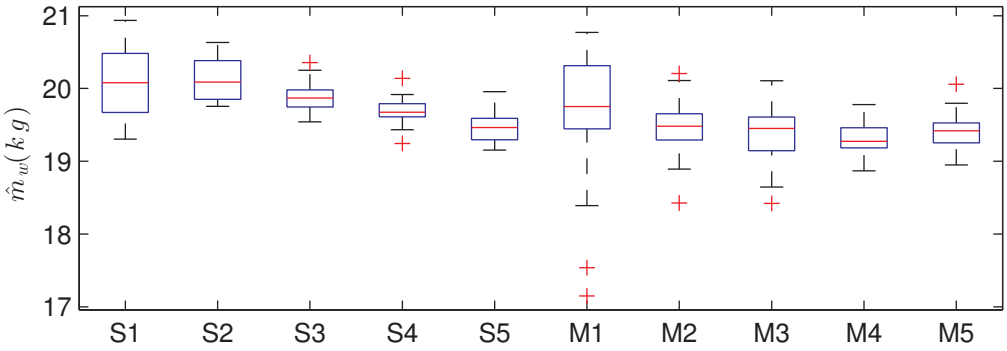

Figure 4-6: Box plot of the estimated mass of the weight over all perturbation profiles. The mass was estimated as $\hat{m}_w = \ddot{x}_w \backslash F_y$.

4-1-3 Model simulation

Evaluation of parameter estimates When the Wristalyzer parameters were used to describe the properties of the ankle joint, θ_{Asim} matched well the measured θ_A from the treadmill experiment. When using the TEP-SIPE parameters , θ_{Asim} did not match θ_A and amplified during the course of the simulation (Figure 4-7). When perturbations were applied less frequently, θ_{Asim} amplified less, but did not follow θ_A (Figure 4-8).
The opposite was found when comparing the simulated and measured ankle torque. The TEP-SIPE parameters could describe τ_A calculated with inverse dynamics but the Wristalyzer parameters were unable to do so (Figure 4-9).
This contrast is visible when comparing the VAFs for θ_{Asim} and τ_{Asim} (Figure 4-10 and Figure 4-11). Using the TEP-SIPE parametes gives high VAF for τ_{Asim} but not for θ_{Asim}. Using the Wristalyzer parameter gives high VAF for θ_{Asim} but not for τ_{Asim}. Only examples from two datsets are shown in this subsection, with the results from all datasets presented in Appendix B.

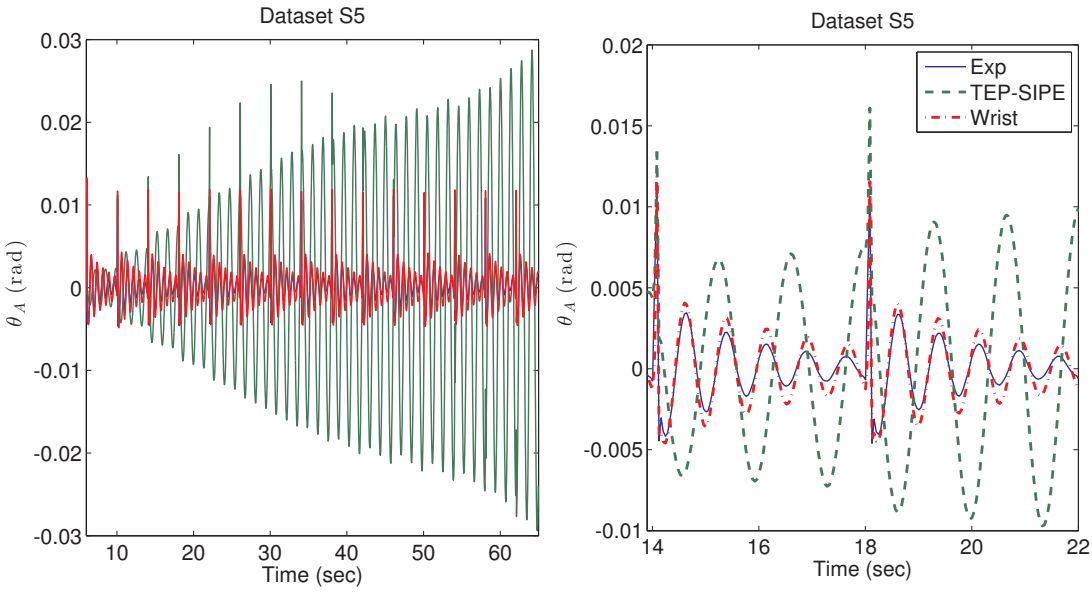

(a) Complete simulation

(b) Short window of the simulation

Figure 4-7: Simulated θ_{Asim} using sinusoidal perturbations with the velocity amplitude of 0.5 m/s. Perturbations were applied every 4 sec. Wristalyzer parameters: I = 0.015, B = 0.1, K = 10. TEP-SIPE parameters: I = 0.061, B = 0.0015, K = 5.34. **Left:** θ_{Asim} using TEP-SIPE parameters amplifies (green line). θ_{Asim} using Wristalyzer parameters follows measured θ_A from treadmill experiment (red line). **Right:** Measured θ_A (blue solid line), θ_{Asim} using TEP-SIPE parameters (green dashed line), θ_{Asim} using Wristalyzer parameters (red dashed-dotted line)

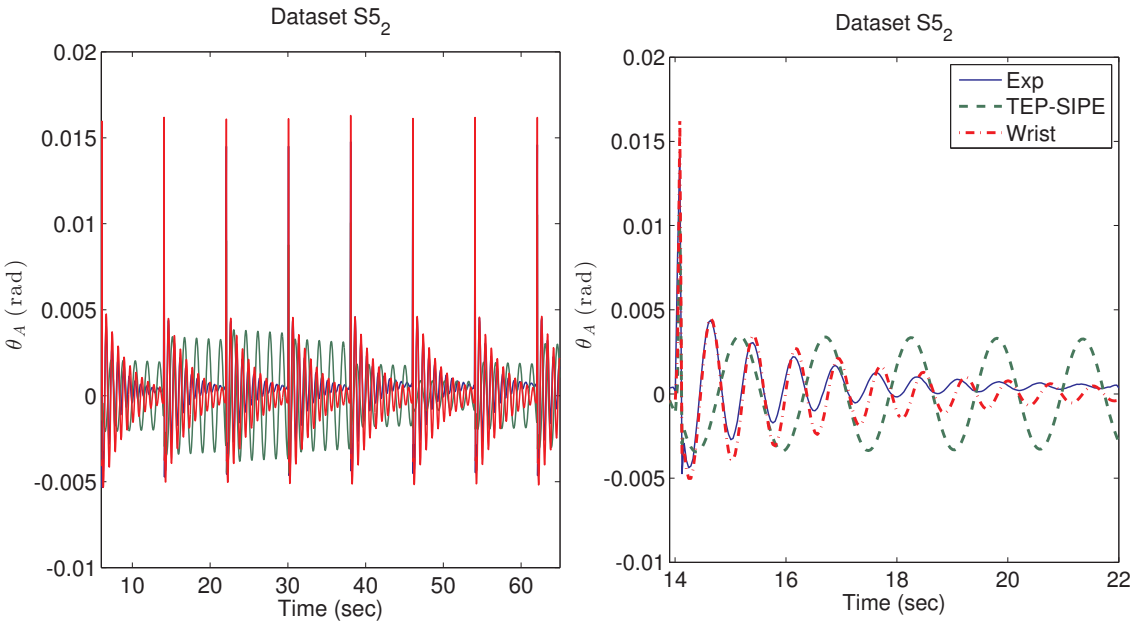

(a) Complete simulation **(b)** Short window of the simulation

Figure 4-8: Simulated θ_{Asim} when sinusoidal perturbations with the velocity amplitude of 0.5 m/s were applied every 8 sec. Wristalyzer parameters: I = 0.015, B = 0.1, K = 10. TEP-SIPE parameters: I = 0.061, B = 0.0137, K = 4.53. **Left**: θ_{Asim} using TEP-SIPE parameters (green line). θ_{Asim} using Wristalyzer parameters (red line). **Right**: Measured θ_A (blue solid line), simulated θ_{Asim} using TEP-SIPE parameters (green dashed line) and Wristalyzer parameters (red dashed-dotted line)

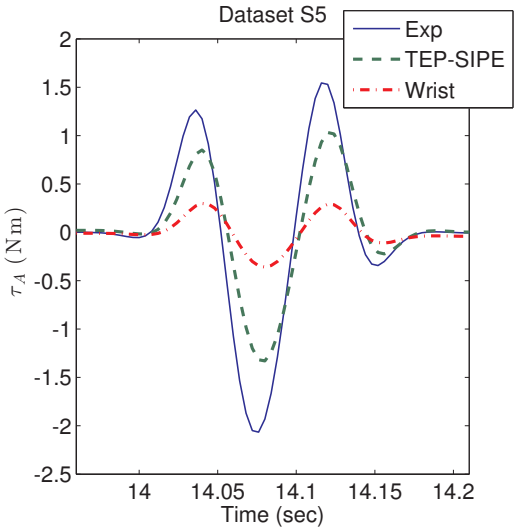

Figure 4-9: τ_A calculated with inverse dynamics (blue solid line), τ_{Asim} simulated with TEP-SIPE parameters (green dashed line) and with Wristalyzer parameters (red dashed-dotted line). Sinusoidal perturbations with velocity amplitude of 0.5 m/s were applied in the simulation.

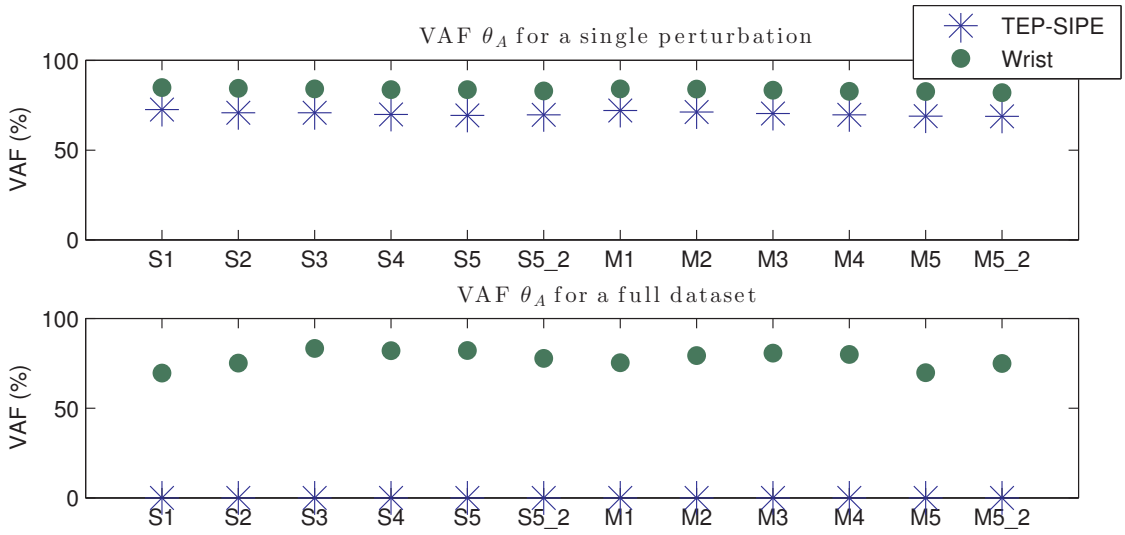

Figure 4-10: VAF for the measured τ_A and simulated τ_{Asim} for a single perturbation

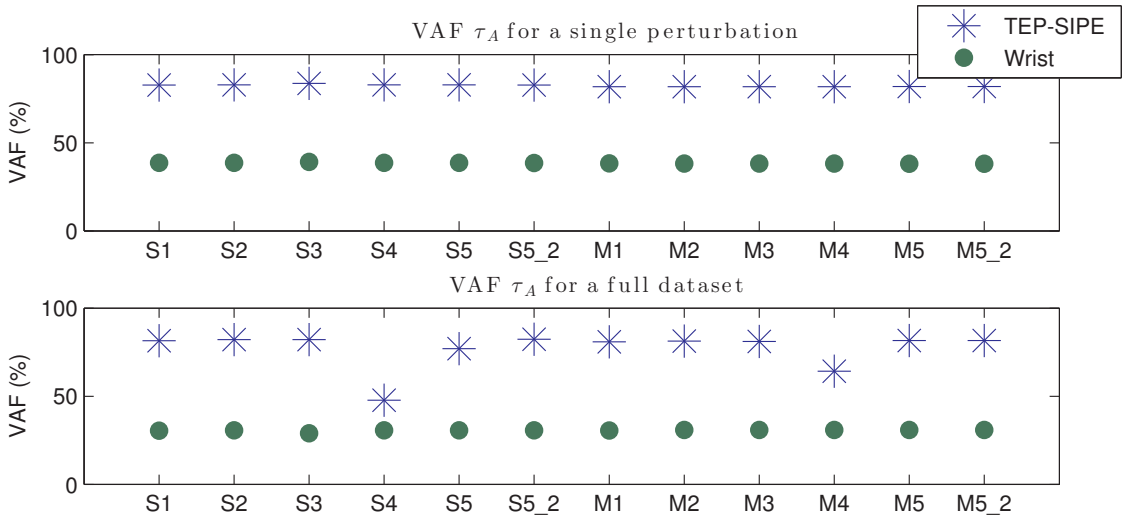

Figure 4-11: VAF for the measured τ_A and simulated τ_{Asim} for a full dataset

Sensitivity to noise When the TEP-SIPE method was applied in a simulation of the treadmill experiment, the estimated parameters matched the true model parameters perfectly. However, when adding measurement noise to the simulated data, the estimated parameters no longer matched the true model parameters.

For all combinations of measurement noise, the quality of the estimated parameters appeared to be good. The SEM values were low for all parameters and for all combinations of noise. VAFs were high when comparing the τ_{Asim} without noise and the $\hat{\tau}_{Asim}$ estimated from the noisy data. (Table 4-4).
For all configurations of noise, the inertia $\hat{I}$ was estimated 2.6 times bigger than the I parameter of the model. The estimated damping $\hat{B}$ was only $\frac{1}{3}$ of the true B parameter of the model. For the stiffness $\hat{K}$, the parameters were also smaller than the true model parameter but differed depending on the noise configuration.
Adding noise to τ_{Asim} resulted in parameters estimated with a high standard deviation, with the biggest deviation for the smallest perturbation amplitudes. The standard deviation of the estimation decreased when noise was only added to θ_{Asim}. Varying the SNR had no clear effect on the parameter estimation (Figure 4-12). Overall, the parameters were lower than the true model parameters. Cross-validation using the parameter estimates to predict the τ_{Asim} gave the highest VAFs when measurement noise had only been added to θ_{Asim}.

		Measurement noise		
	No noise	τ_{Asim}	θ_{Asim}	τ_{Asim} and θ_{Asim}
$\hat{I}$ [Nms^2/rad]	0.015	0.039	0.039	0.039
$\hat{B}$ [Nms/rad]	0.1	0.031	0.027	0.029
$\hat{K}$ [Nm/rad]	10	2.963	0.028	0.011
SEM of I [-]	0	$8{\cdot}10^{-4}$	$1\cdot10^{-4}$	$7{\cdot}10^{-4}$
SEM of B [-]	0	0.032	0.006	0.035
SEM of K [-]	0	1.915	0.039	0.152
$\overline{VAF}_{\tau_A}$ of perturbation [%]	100	96	96	96
VAF_{τ_A} of full dataset [%]	100	96	96	96
$\overline{VAF}_{\tau_A} C-V$ of full dataset [%]	–	72	99	71
$\overline{VAF}_{\theta_A}$ of perturbation [%]	–	90	0	0
VAF_{θ_A} of full dataset [%]	–	0.6	0	0

Table 4-4: The parameter estimates using the TEP-SIPE method. SEM values are low for all parameters. VAF_{τ_A} values are high when comparing τ_{Asim}. When the estimated parameters are used to predict the motion of the dummy, the VAF_{θ_A}s for θ_{Asim} are low.

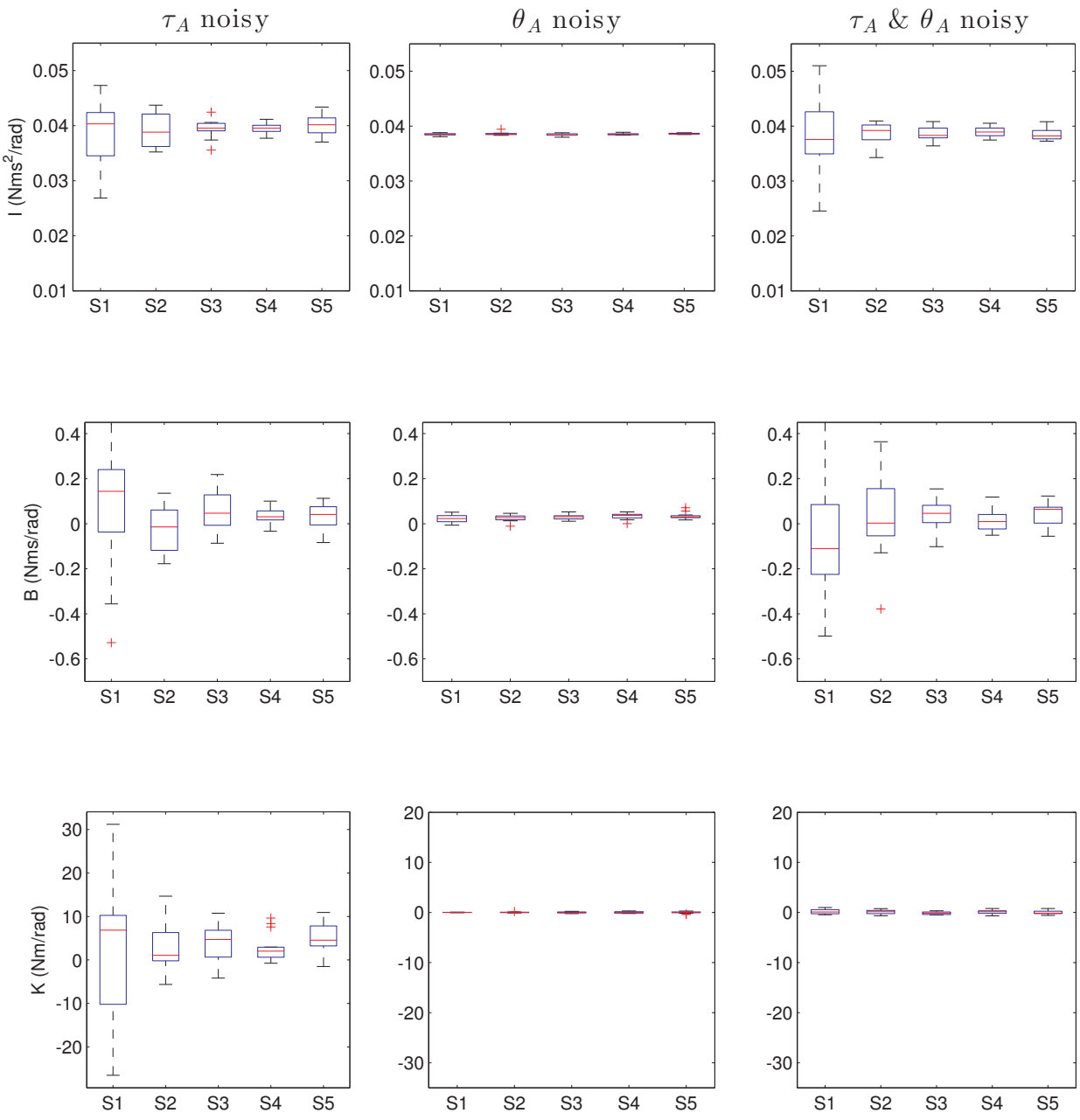

Figure 4-12: The estimated parameters when sinusoidal perturbations the velocity amplitude of 0.1-0.5 m/s were applied in the simulation (denoted as S1-S5 on the x-axis). All datasets had a SNR of 20 dB. The true model parameters were I = 0.015, B = 0.1, K = 15. Left: Measurement noise added to τ_{Asim}. Center: Measurement noise added to θ_{Asim}. Right: Measurement noise added to τ_{Asim} and θ_{Asim}.

4-2 TEP-SIPE Application

The transient endpoint perturbations are very well visible in the recorded ankle angle and torque data (Figure 4-13). The delayed onset of the muscular activity is visible when it is compared to the actual onset of the perturbation (4-14).

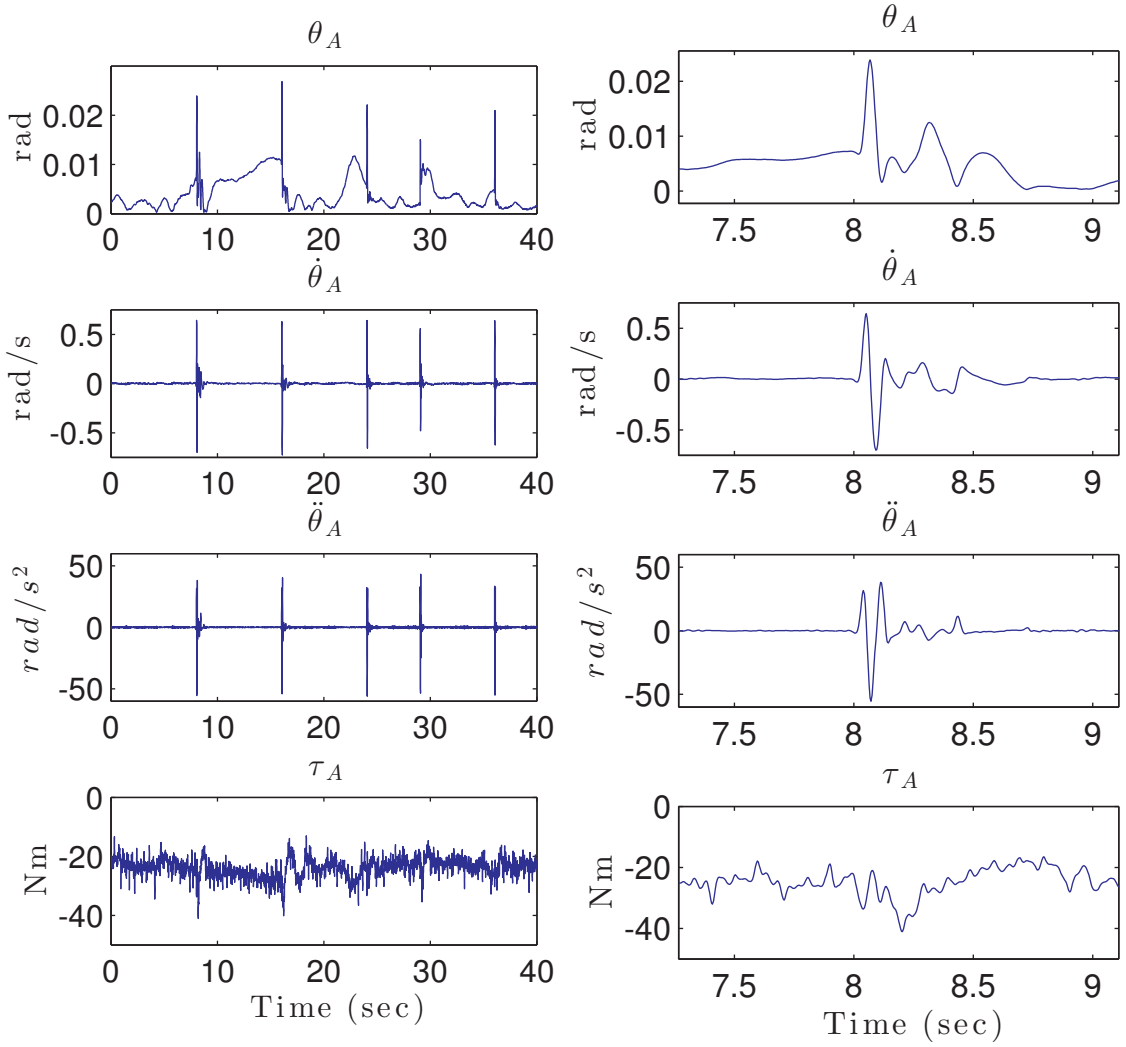

(a) Full trial

(b) One perturbation

Figure 4-13: Angular angle θ_A, velocity $\dot{\theta}_A$, acceleration $\ddot{\theta}_A$ measured from the motion tracking system. Ankle torque τ_A calculated from inverse dynamics. The data is from a standing trial applying sinusoidal perturbations with the amplitude of 0.4 m/s. The subject was instructed to maintain a relaxed position.

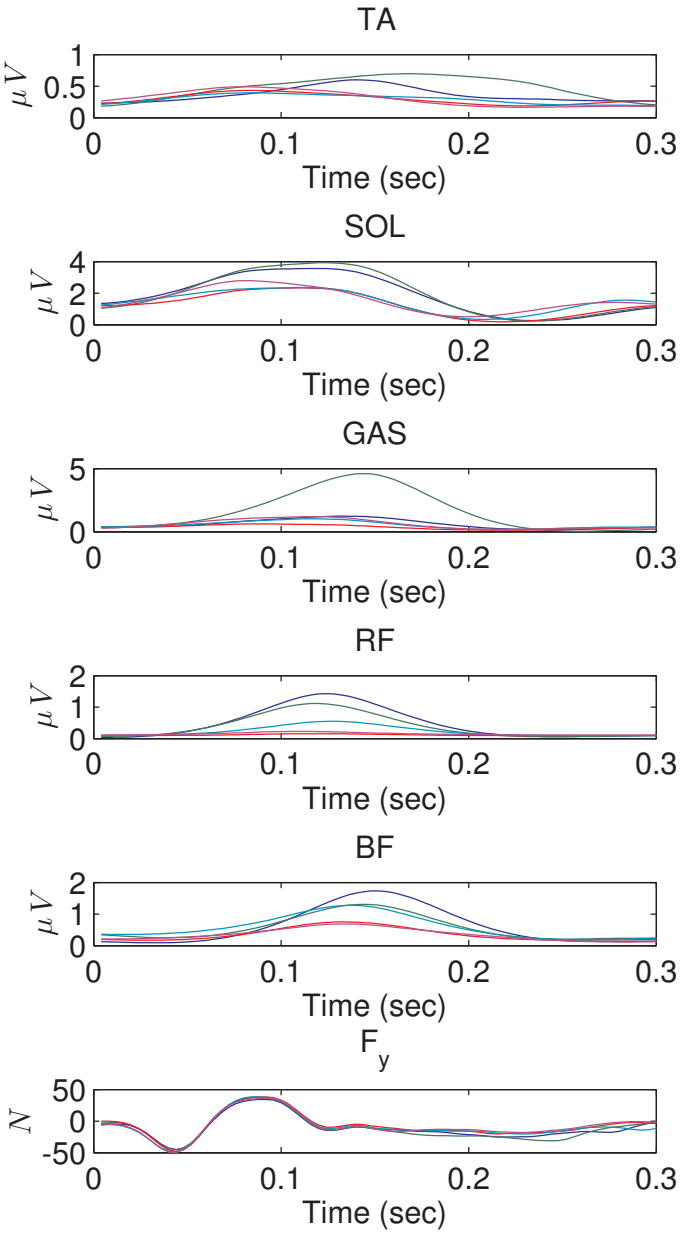

Figure 4-14: The plots starts at the onset of every perturbation and shows the EMG responses for all five muscle groups measured in pilot study. Bottom: The measured force F_y from the treadmill.

Chapter 5

Discussion and Outlook

This study evaluated the ability of TEP-SIPE method to identify joint impedance. The method consists of applying transient endpoint perturbations using an instrumented treadmill. The recorded data is processed in time-domain by fitting short data segments, including only the perturbation, to a model of the system's dynamics.
The validation was performed in the three steps. First, an established method based on perturbation experiments using the Wristalyzer was used to identify joint impedance of a single-joint ankle dummy. Second, the TEP-SIPE method based on transient endpoint perturbations using an instrumented treadmill was used to identify these parameters as well. Third, the treadmill experiment was simulated using a SimMechanics model of the ankle dummy. The influences from the instrumented treadmill used for the experiments were evaluated in a weight experiment. The weight experiment was an important step to investigate the reliability of the recorded forces and moment and to see whether force recordings from an unloaded belt were sufficient to describe the dynamics of the treadmill. Finally, the TEP-SIPE method was applied in a pilot study with a human subject standing on a treadmill.

Influences from treadmill dynamics

The weight experiment demonstrated that the effects from treadmill dynamics are influencing the results of the TEP-SIPE method and must be removed. The mean forces $\boldsymbol{F_{y0}}$ recorded with the empty treadmill could not be simply subtracted from the forces recorded with the the weight and ankle dummy. Fitting the forces of the treadmill to a simple second order model was not sufficient either, indicating that the dynamics are more complex. When trying to remove the unwanted effects from the treadmill with a lower cutoff frequency of 10 Hz, $\boldsymbol{F_{y0}}$ resembled $\boldsymbol{\Delta F_y}$ qualitatively, but not quantitatively (Figure 5-1).

The difference was highest at maximum velocity of the treadmill and increased with increasing perturbation amplitude. It appears that the recorded $\boldsymbol{F_y}$ does not increase proportionally to

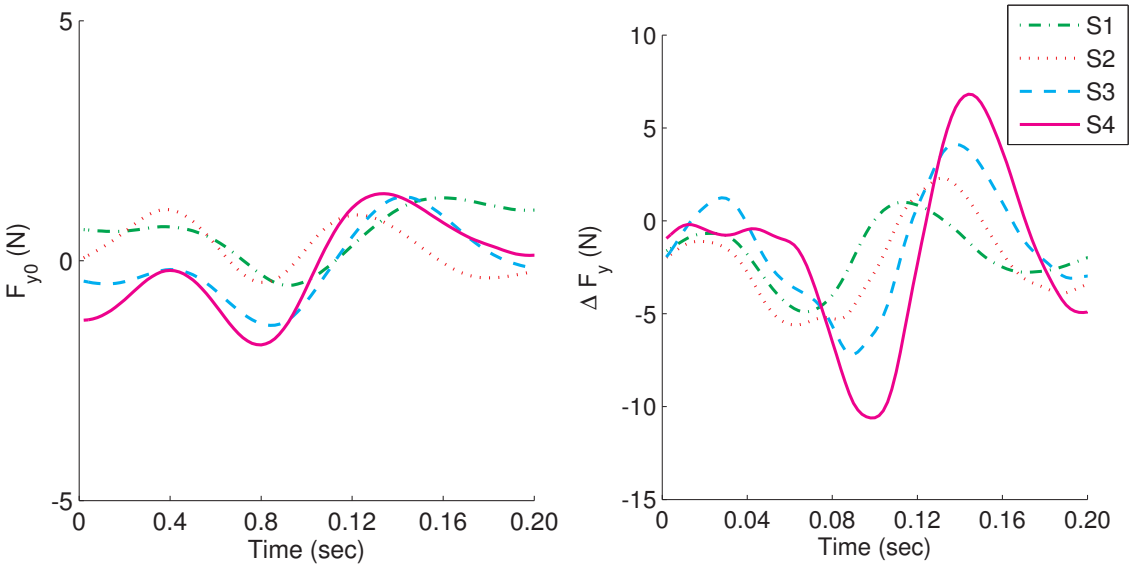

(a) The mean F_{y0} over all perturbations

(b) The mean difference ΔF_y over all perturbations

Figure 5-1: a) Forces measured with the empty treadmill b) The difference of forces measured in the weight experiment. The forces were filtered with a 4^{th} order Butterworth filter with a lowpass cutoff frequency of 10 Hz. Only 4 perturbation profiles are shown; sinusoidal perturbations with velocity amplitude 0.1-0.4 m/s denoted as S1 - S4.

the increased perturbation amplitude. That might explain why the mass estimation lowered as the perturbation amplitude increased.

Interpretation of the quality of parameter estimates

The joint parameters of the ankle dummy could be accurately estimated with the Wristalyzer, as was seen by high VAFs and low SEM values. The stiffness K had higher SEM-values than the I and B parameters. This might be explained by poor frequency resolution on low frequencies, where the stiffness is dominating. The perturbation signal in the Wristalyzer contained a frequency bandwidth of 1-20 Hz, but parameters were estimated on a lower bandwidth.That was done to account for potential short-comings in the fixation of the dummy. A transition line was visible at frequencies above 9 Hz, indicating influences from the fixation strap. That frequency was thus chosen as the upper threshold of the frequency band used for the parameter estimation. The parameter boundaries were tuned to avoid reaching local minimum with the optimization algorithm. Using different boundaries, parameters were also estimated which gave high VAFs, but cross-validation gave poor results. The uniqueness of the current set of parameters was validated in the model simulation which showed that the parameters were able to describe the measured angular movement of the real dummy.

It is questionable whether the inertia parameter estimated with the Wristalyzer and TEP-SIPE methods are directly comparable. The ankle dummy was tested in two different configurations. In the Wristalyzer, the dummy's foot pivoted about the ankle joint while the rod

remained fixed to the arm rest. In the treadmill experiment, the rod pivoted about its end-point over the ankle joint while the foot was fixed to the treadmill. If the moment of inertia is calculated using the mass and moment arm of the segment pivoting about the rotation point, different values are expected.
The point of rotation might pose another limitation. In the Wristalyzer, the ankle dummy was tightly fastened above a fixed rotation point. In the simulation, the ankle joint also defined as a single ankle joint with a fixed rotation point. However, in the treadmill experiment, the ankle dummy is less constrained. It is possible that the point of rotation translates slightly during the experiment, thus influencing the further the parameter estimate.

Using the TEP-SIPE method resulted in set of parameters with high VAF and low SEM values. However, model simulation with the TEP-SIPE parameters clearly showed that the measured motion of the dummy was not matched. It appears that the method is prone to reach local minima, where the parameters are not physically meaningful and a unique solution is not found. Furthermore, using the VAF and SEM as a measure of parameter quality seems an insufficient measure. Further measures are needed as was shown with the model simulation.

It is important to keep in mind the primary goal of the TEP-SIPE method, which is to estimate physically meaningful parameters for the use of bio-inspired control of prosthetic devices or for therapeutic assessment of patients suffering from UMND. The TEP-SIPE parameters could describe the torque trajectory for a impedance controlled prosthetic device, but one must note that the parameters might not be physically meaningful. As for the therapeutic assessment, the TEP-SIPE method could reveal the absolute difference between the healthy subjects and patients when using the same experimental setup and post-processing steps. As such, it can therefore assist in differentiating between healthy and impaired joint behavior. However, the method might not be applicable when using more than one experimental setup (i.e. measuring healthy subjects and patients in a separate setup) which further limits the application of the method.

The effects of varying perturbation profiles

The quality of the parametric fit suggested that sinusoidal perturbation profiles were more suitable than minimal jerk profiles. Furthermore, higher perturbation velocity amplitudes resulted in parameters estimated more consistently (i.e with a lower standard deviation).
Accurate onset detection of the perturbations is very important when estimating parameters with the TEP-SIPE method. Sinusoidal perturbations profiles are better repeatable than minimum jerk profiles, which facilitates perturbation detection in the post-processing. Higher perturbation velocity amplitudes are also more visible, which makes automatic onset detection easier.

Sensitivity to measurement noise

The simulation showed that measurement noise influences the parameter estimation, where parameters were incorrectly estimated for all configurations of noise. Without measurement noise, the TEP-SIPE algorithm was able to estimate the model parameters perfectly. Adding

measurement noise, all parameter estimates were incorrect. An interesting finding was that despite incorrect parameter estimation, the VAFs were high and SEM values were low. This was in line with the experimental results, where the parameters estimated with the TEP-SIPE gave good fit although they were not correct. This further indicates that measurement noise, or more importantly, the treadmill dynamics might be included in the parametric fitting for the of the treadmill data.

The force data is influenced by measurement noise in the real experiment. The motion recordings are less influenced by measurement noise. This is an important aspect when calculating the ankle torque from inverse dynamics. One could either use equations of motion for the foot or the leg segment to derive the torque. The equations for the foot include the treadmill forces and might therefore result in noisy torque. The equations for the leg include only the recorded motion of the leg, which might reduce the effect of noise in the ankle torque.

The effects of filtering

It is possible that influences from measurement noise and treadmill dynamics can be circumvented to some extent with an adequate choice of filter. All experimental and simulated data was filtered with a 4^{th} order bi-directional Butterworth filter with a cutoff frequency of 20 Hz. Due to the number of experimental setups and protocols it was important to be consistent in the choice of filter to reduce the number of uncertainties. The data had to be carefully synchronized and a bi-directional filter was therefore chosen since it does not shift in data. However, since it is a recursive filter, it introduces a slight distortion in the data which might influence the results. Using a uni-directional filter causes a shift in the data. As a result, filtering with both uni-and bidirectional filters must be done with care to ensure that the data stays synchronized.

Applying TEP-SIPE in human experiments

The pilot study was an important point in the future direction, although the data evaluation was not part of the thesis. It was among the first experiments aiming to identify joint impedance during standing using only transient endpoint perturbations from an instrumented treadmill.
The treadmill experiments with the ankle-dummy might give conditional support of the use of the TEP-SIPE method, but they give no proof. The joint properties of the single-joint ankle dummy can be described with a simple, second order model. The joint properties of a multi-joint human require a more complex model incorporating the neural reflexive pathways, time delays and activation dynamics. Therefore, validating the TEP-SIPE method with the ankle dummy might not apply for the human. To assume that the human behaves like an inverted pendulum during standing is thus a crude simplification and disregards many important aspects. The mechanical coupling of the ankle, knee and hip joints will inevitably influence the impedance estimates. The movements from the upper body will influence the movements of the lower body and vice versa [26].
Still, the pilot study was important to evaluate whether transient endpoint perturbations are sufficient to elicit reflexes at all. Perturbations can be well distinguished in the force and

motion data. Furthermore, the EMG recordings from the pilot study showed distinct muscular reaction which might indicate that reflexes are elicited. Differentiation into intrinsic and reflexive components might therefore be possible.

Future research

The next steps should focus on carefully quantifying and modeling the treadmill dynamics so that they can be separated from the joint dynamics. Only then is it possible to continue the validation of TEP-SIPE method and investigate if the method returns a unique set of physiologically meaningful parameters. It is possible that a more sophisticated calibration matrix accounting for the effects from the treadmill dynamics can partly solve this problem. Another possibility is to model the dynamics of the treadmill in a similar way as has been done in a different study [34].

As for the conceptual feasibility of applying transient endpoint perturbation to identify joint impedance, some studies suggest that an independent perturbation is needed for each degree of freedom [26, 35]. A model simulation, similar to the one used in the thesis, might be useful to shed a light on whether multiple perturbations are needed in a real human experiment. The single-joint model can be extended to a multi-joint model, incorporating a neuro-musculoskeletal model to describe the joint properties. Knowing all the parameters of the model, the simulation could indicate whether increasing the number of perturbations improves the parameter estimates. Different points of application could be tested as well as different perturbation timings (e.g. perturbations during swing phase). The simulation study can therefore provide meaningful information while simultaneously reducing the experimental effort. The model simulation could also be a useful tool to optimize the type of filter used in the post-processing. Ideally, the unwanted effects from the treadmill should be removed without excluding the dynamic response of the joint.

The experimental data from the pilot study should be analyzed, with the aim to quantify the intrinsic and reflexive components of the joint impedance. The EMG can be used as a measure to determine the onset of reflexes.

Chapter 6

Conclusion

This goal of this study was to validate the ability of TEP-SIPE method to identify joint impedance. The method consists of applying transient endpoint perturbations using an instrumented treadmill. The recorded data is processed in time-domain by fitting short data segments, including only the perturbation, to a model of the system's dynamics.

The TEP-SIPE method was able to precisely estimate joint parameters with high VAFs and low SEM values. However, the parameters were not physically meaningful and did not match true parameters estimated in the Wristalyzer. Forward simulation further demonstrated that the measured motion of the dummy could not be matched when using the TEP-SIPE parameters to describe the joint properites.
This could be explained by the influences from the treadmill dynamics. The weight experiment showed that effects from the treadmill dynamics were substantial and could not be easily subtracted from the data. Forward simulation showed that the TEP-SIPE method is sensitive to measurement noise and is prone to reach local minima. The use of VAF and SEM values to determine the quality of the fit might be thus be insufficient. In the pilot study, the transient endpoint perturbations were clearly distinguished in motion and EMG data, indicating that further evaluation of the data is possible.

In general, the TEP-SIPE method could not be validated with experiments, i.e. the uniqueness of the estimated parameters could not be guaranteed. However, the limitations of the method and the available experimental setup were carefully identified. Thorough guideline for the TEP-SIPE method has been developed which facilitates the use of the method and sharpens the goal for further research.

Appendix A

Data post-processing

This section presents the schemes for post-processing the Wristalyzer and treadmill data. The schemes can be interpreted as possibility pathways, showing alternative options for each part of the post-processing. All options were considered during the course of this Master thesis, before choosing the path shown with red arrows.

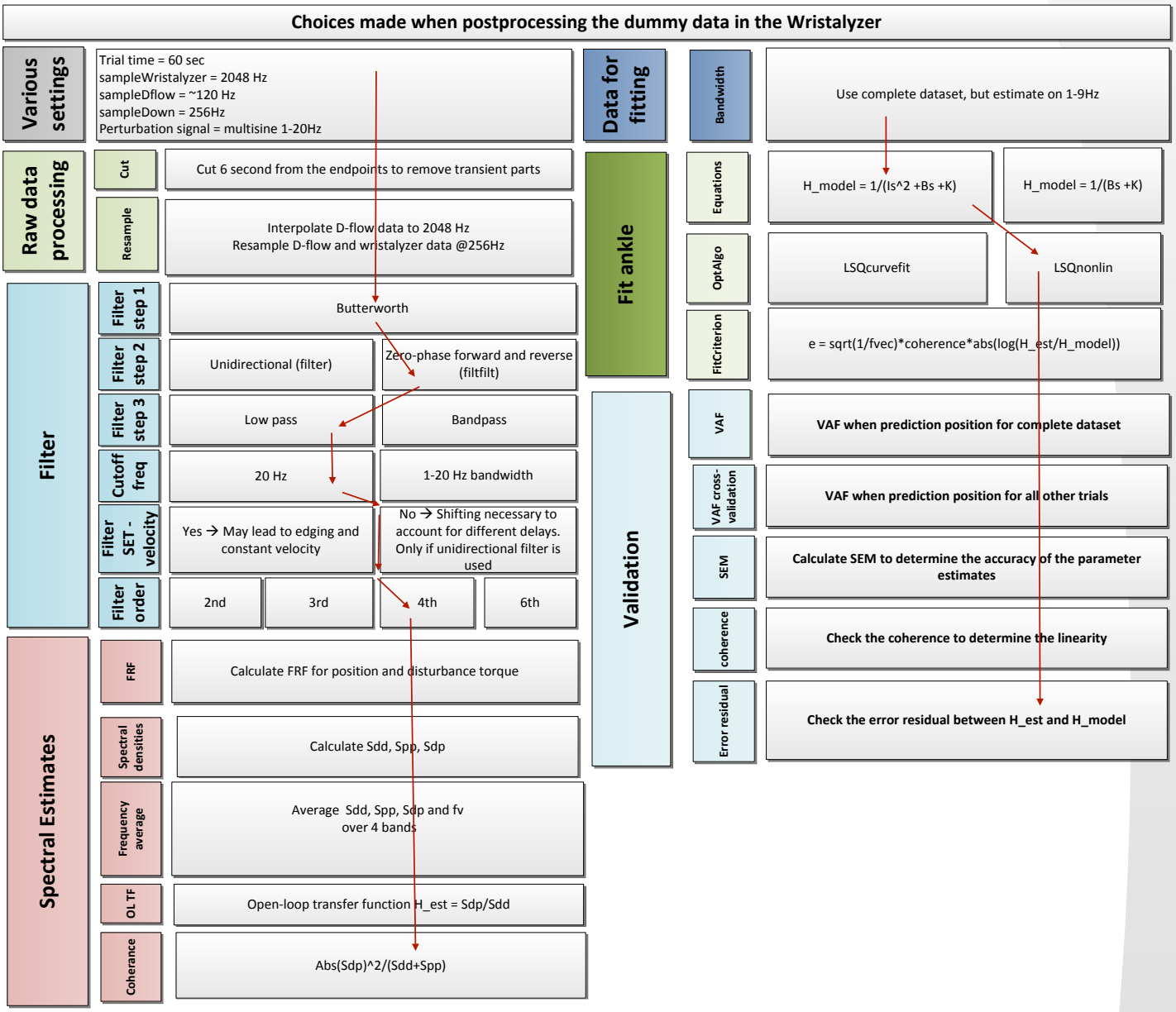
Choices made when postprocessing the dummy data in the Wristalyzer
Various settings
Trial time = 60 sec
sampleWristalyzer = 2048 Hz
sampleDflow = ~120 Hz
sampleDown = 256Hz
Perturbation signal = multisine 1-20Hz
Raw data processing
Cut
Cut 6 second from the endpoints to remove transient parts
Resample
Interpolate D-flow data to 2048 Hz
Resample D-flow and wristalyzer data @256Hz
Filter
Filter step 1
Butterworth
Filter step 2
Unidirectional (filter)
Zero-phase forward and reverse (filtfilt)
Filter step 3
Low pass
Bandpass
Cutoff freq
20 Hz
1-20 Hz bandwidth
Filter SET - velocity
Yes → May lead to edging and constant velocity
No → Shifting necessary to account for different delays. Only if unidirectional filter is used
Filter order
2nd
3rd
4th
6th
Spectral Estimates
FRF
Calculate FRF for position and disturbance torque
Spectral densities
Calculate Sdd, Spp, Sdp
Frequency average
Average Sdd, Spp, Sdp and fv over 4 bands
OL TF
Open-loop transfer function H_est = Sdp/Sdd
Coherance
Abs(Sdp)^2/(Sdd+Spp)
Data for fitting
Bandwidth
Use complete dataset, but estimate on 1-9Hz
Fit ankle
Equations
H_model = 1/(Is^2 +Bs +K)
H_model = 1/(Bs +K)
OptAlgo
LSQcurvefit
LSQnonlin
FitCriterion
e = sqrt(1/fvec)*coherence*abs(log(H_est/H_model))
Validation
VAF
VAF when prediction position for complete dataset
VAF cross-validation
VAF when prediction position for all other trials
SEM
Calculate SEM to determine the accuracy of the parameter estimates
coherence
Check the coherence to determine the linearity
Error residual
Check the error residual between H_est and H_model

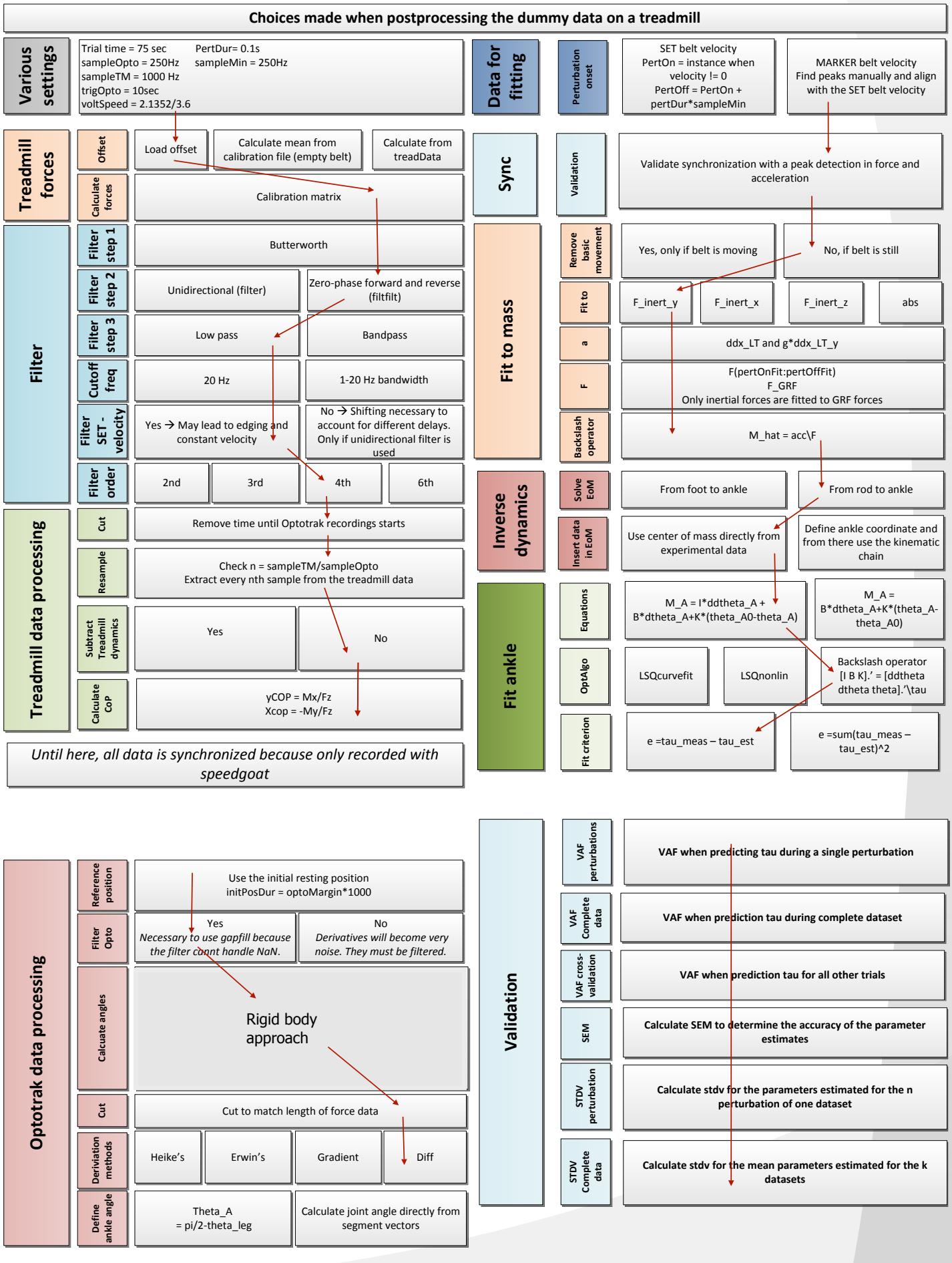
Choices made when postprocessing the dummy data on a treadmill
Various settings
Trial time = 75 sec
sampleOpto = 250Hz
sampleTM = 1000 Hz
trigOpto = 10sec
voltSpeed = 2.1352/3.6
PertDur= 0.1s
sampleMin = 250Hz
Treadmill forces
Offset
Load offset
Calculate mean from calibration file (empty belt)
Calculate from treadData
Calculate forces
Calibration matrix
Filter
Filter step 1
Butterworth
Filter step 2
Unidirectional (filter)
Zero-phase forward and reverse (filtfilt)
Filter step 3
Low pass
Bandpass
Cutoff freq
20 Hz
1-20 Hz bandwidth
Filter SET - velocity
Yes → May lead to edging and constant velocity
No → Shifting necessary to account for different delays. Only if unidirectional filter is used
Filter order
2nd
3rd
4th
6th
Treadmill data processing
Cut
Remove time until Optotrak recordings starts
Resample
Check n = sampleTM/sampleOpto
Extract every nth sample from the treadmill data
Subtract Treadmill dynamics
Yes
No
Calculate CoP
yCOP = Mx/Fz
Xcop = -My/Fz
Until here, all data is synchronized because only recorded with speedgoat
Data for fitting
Perturbation onset
SET belt velocity
PertOn = instance when velocity != 0
PertOff = PertOn + pertDur*sampleMin
MARKER belt velocity
Find peaks manually and align with the SET belt velocity
Sync
Validation
Validate synchronization with a peak detection in force and acceleration
Fit to mass
Remove basic movement
Yes, only if belt is moving
No, if belt is still
Fit to
F_inert_y
F_inert_x
F_inert_z
abs
a
ddx_LT and g*ddx_LT_y
F
F(pertOnFit:pertOffFit)
F_GRF
Only inertial forces are fitted to GRF forces
Backslash operator
M_hat = acc\F
Inverse dynamics
Solve EoM
From foot to ankle
From rod to ankle
Insert data in EoM
Use center of mass directly from experimental data
Define ankle coordinate and from there use the kinematic chain
Fit ankle
Equations
M_A = I*ddtheta_A + B*dtheta_A+K*(theta_A0-theta_A)
M_A = B*dtheta_A+K*(theta_A-theta_A0)
OptAlgo
LSQcurvefit
LSQnonlin
Backslash operator [I B K].' = [ddtheta dtheta theta].'\tau
Fit criterion
e =tau_meas – tau_est
e =sum(tau_meas – tau_est)^2
Optotrak data processing
Reference position
Use the initial resting position
initPosDur = optoMargin*1000
Filter Opto
Yes
Necessary to use gapfill because the filter cannt handle NaN.
No
Derivatives will become very noise. They must be filtered.
Calcuate angles
Rigid body approach
Cut
Cut to match length of force data
Derivation methods
Heike's
Erwin's
Gradient
Diff
Define ankle angle
Theta_A = pi/2-theta_leg
Calculate joint angle directly from segment vectors
Validation
VAF perturbations
VAF when predicting tau during a single perturbation
VAF Complete data
VAF when prediction tau during complete dataset
VAF cross-validation
VAF when prediction tau for all other trials
SEM
Calculate SEM to determine the accuracy of the parameter estimates
STDV perturbation
Calculate stdv for the parameters estimated for the n perturbation of one dataset
STDV Complete data
Calculate stdv for the mean parameters estimated for the k datasets

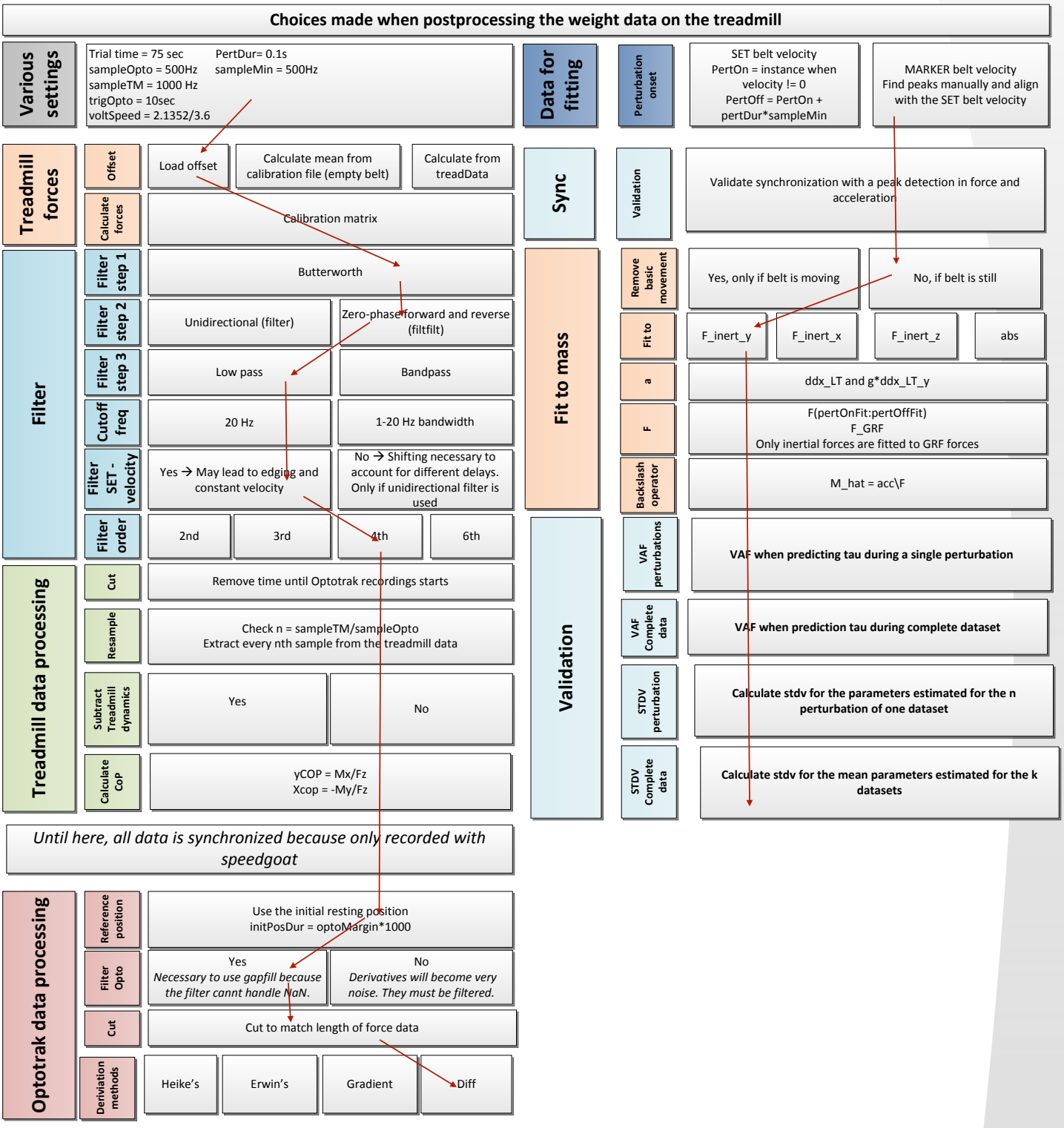
Choices made when postprocessing the weight data on the treadmill
Various settings
Trial time = 75 sec
sampleOpto = 500Hz
sampleTM = 1000 Hz
trigOpto = 10sec
voltSpeed = 2.1352/3.6
PertDur= 0.1s
sampleMin = 500Hz
Data for fitting
Perturbation onset
SET belt velocity
PertOn = instance when velocity != 0
PertOff = PertOn + pertDur*sampleMin
MARKER belt velocity
Find peaks manually and align with the SET belt velocity
Treadmill forces
Offset
Load offset
Calculate mean from calibration file (empty belt)
Calculate from treadData
Calculate forces
Calibration matrix
Sync
Validation
Validate synchronization with a peak detection in force and acceleration
Filter
Filter step 1
Butterworth
Filter step 2
Unidirectional (filter)
Zero-phase forward and reverse (filtfilt)
Filter step 3
Low pass
Bandpass
Cutoff freq
20 Hz
1-20 Hz bandwidth
Filter SET - velocity
Yes → May lead to edging and constant velocity
No → Shifting necessary to account for different delays. Only if unidirectional filter is used
Filter order
2nd
3rd
4th
6th
Fit to mass
Remove basic movement
Yes, only if belt is moving
No, if belt is still
Fit to
F_inert_y
F_inert_x
F_inert_z
abs
a
ddx_LT and g*ddx_LT_y
F
F(pertOnFit:pertOffFit)
F_GRF
Only inertial forces are fitted to GRF forces
Backslash operator
M_hat = acc\F
Treadmill data processing
Cut
Remove time until Optotrak recordings starts
Resample
Check n = sampleTM/sampleOpto
Extract every nth sample from the treadmill data
Subtract Treadmill dynamics
Yes
No
Calculate CoP
yCOP = Mx/Fz
Xcop = -My/Fz
Validation
VAF perturbations
VAF when predicting tau during a single perturbation
VAF Complete data
VAF when prediction tau during complete dataset
STDV perturbation
Calculate stdv for the parameters estimated for the n perturbation of one dataset
STDV Complete data
Calculate stdv for the mean parameters estimated for the k datasets
Until here, all data is synchronized because only recorded with speedgoat
Optotrak data processing
Reference position
Use the initial resting position
initPosDur = optoMargin*1000
Filter Opto
Yes
Necessary to use gapfill because the filter cannt handle NaN.
No
Derivatives will become very noise. They must be filtered.
Cut
Cut to match length of force data
Deriviation methods
Heike's
Erwin's
Gradient
Diff

Appendix B

Model simulation

This sections shows the output from the simulation, when all perturbation profiles were tested. Each simulation was repeated using two sets of parameters, first with the Wristalyzer parameters and then with the TEP-SIPE parameters. For all perturbation profiles, the Wristalyzer parameters (shown in red) are able to adequately follow the measured angular trajectory from the experiment. The TEP-SIPE parameters were unable to match the measured angular trajectory, and the simulated motion became unstable for some perturbation profiles.

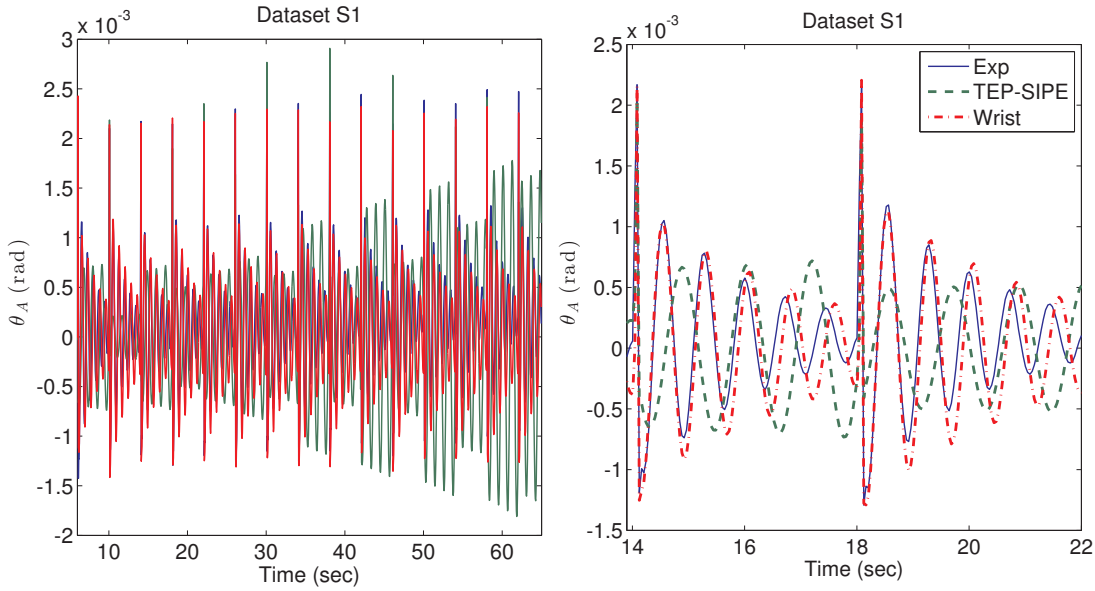

(a) Complete simulation

(b) Short window of the simulation

Figure B-1: Sinusoidal perturbation with velocity amplitude 0.1 m/s

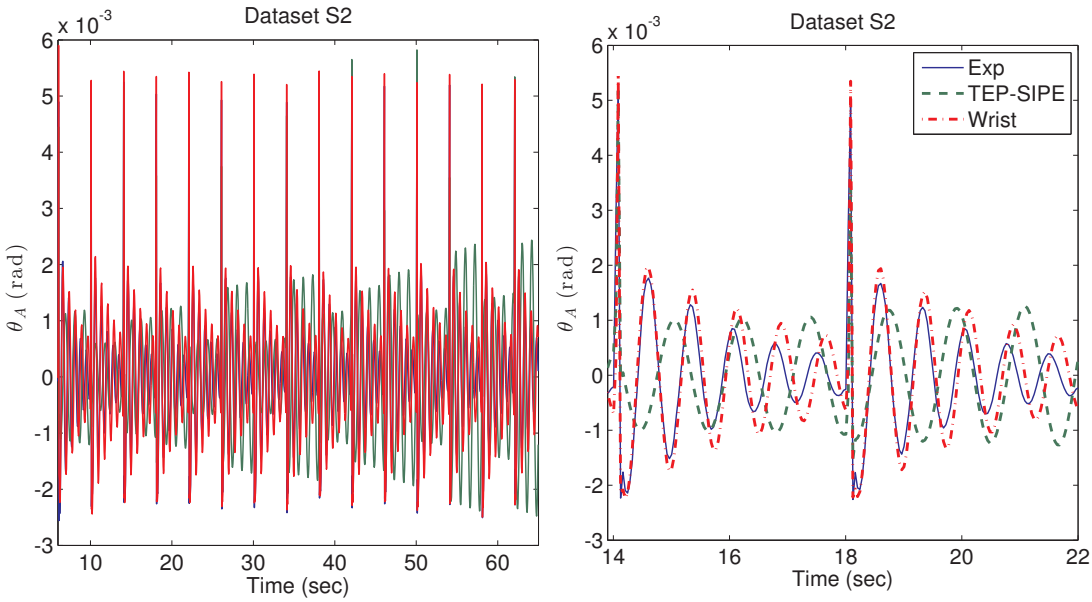

(a) Complete simulation **(b)** Short window of the simulation

Figure B-2: Sinusoidal perturbation with velocity amplitude 0.2 m/s

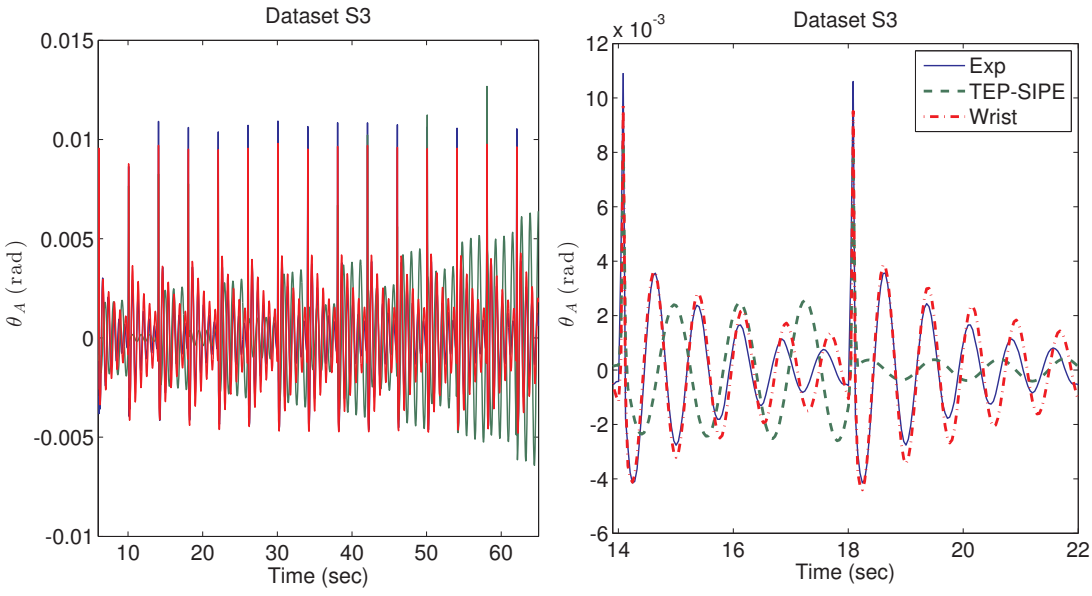

(a) Complete simulation **(b)** Short window of the simulation

Figure B-3: Sinusoidal perturbation with velocity amplitude 0.3 m/s

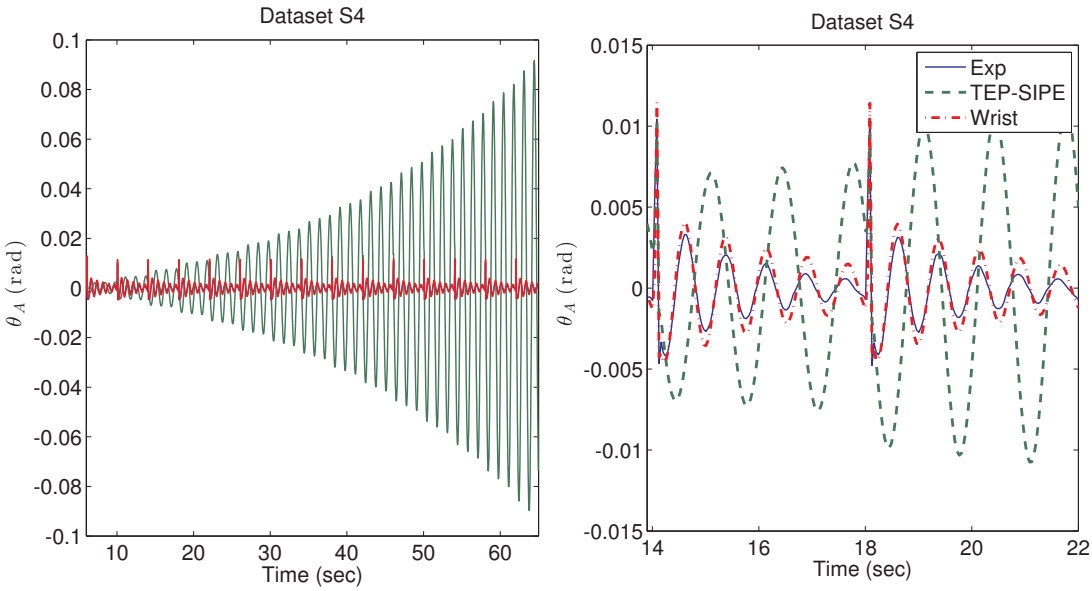

(a) Complete simulation

(b) Short window of the simulation

Figure B-4: Sinusoidal perturbation with velocity amplitude 0.4 m/s

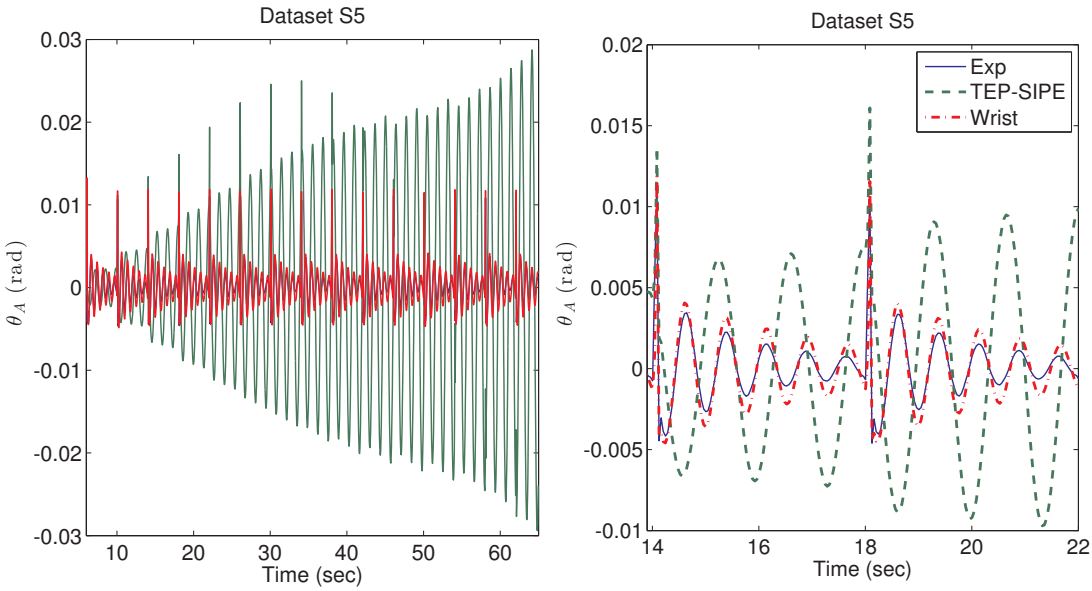

(a) Complete simulation

(b) Short window of the simulation

Figure B-5: Sinusoidal perturbation with velocity amplitude 0.5 m/s

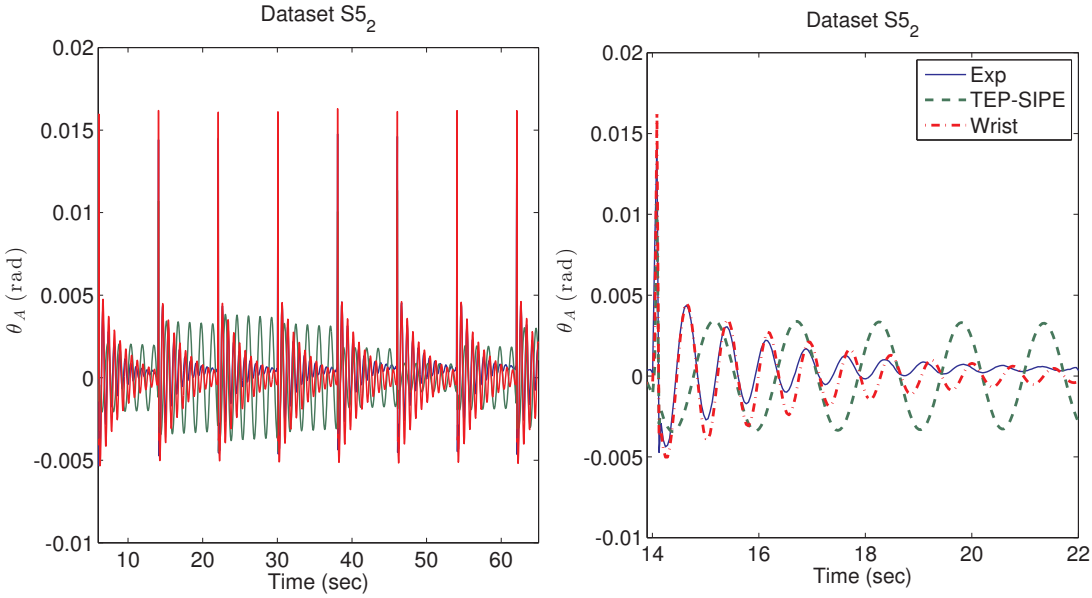

(a) Complete simulation **(b)** Short window of the simulation

Figure B-6: Sinusoidal perturbation with velocity amplitude 0.5 m/s. Perturbation were applied every 8 seconds.

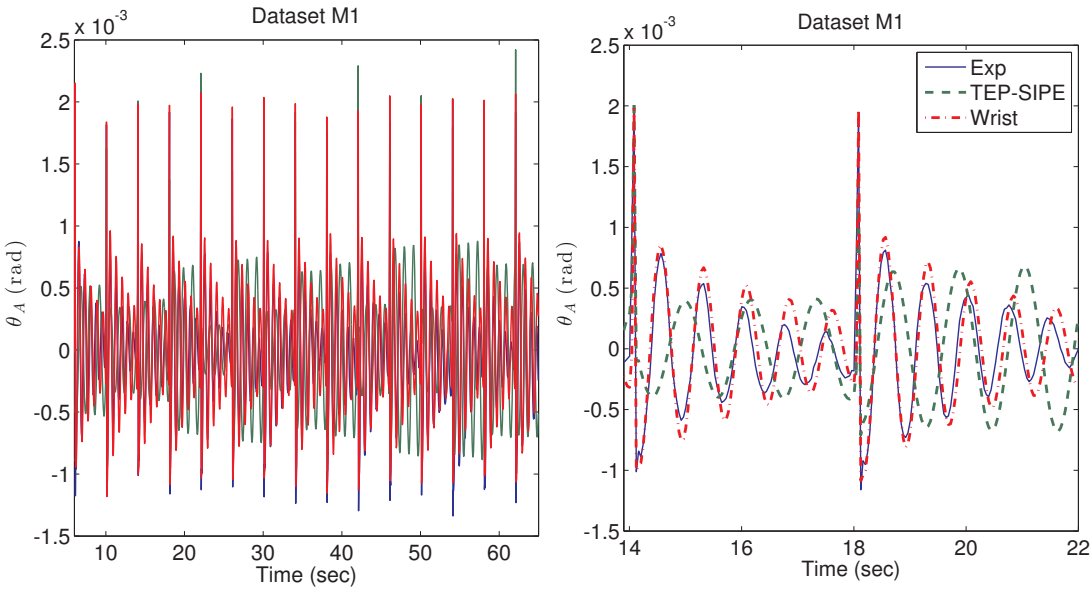

(a) Complete simulation **(b)** Short window of the simulation

Figure B-7: Minimum jerk perturbation with velocity amplitude 0.1 m/s

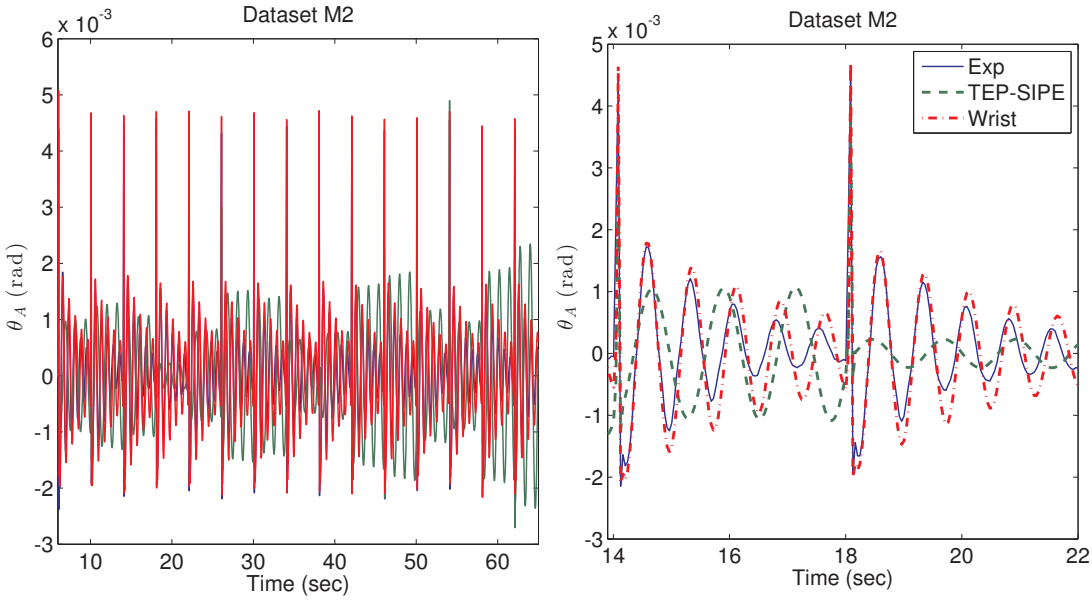

(a) Complete simulation **(b)** Short window of the simulation

Figure B-8: Minimum jerk perturbation with velocity amplitude 0.2 m/s

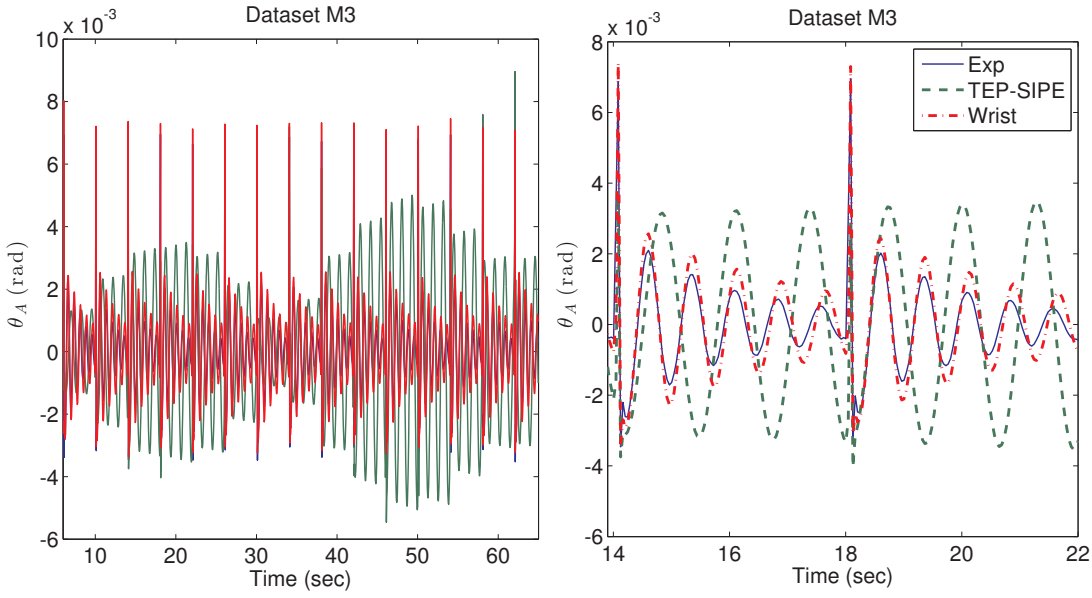

(a) Complete simulation **(b)** Short window of the simulation

Figure B-9: Minimum jerk perturbation with velocity amplitude 0.3 m/s

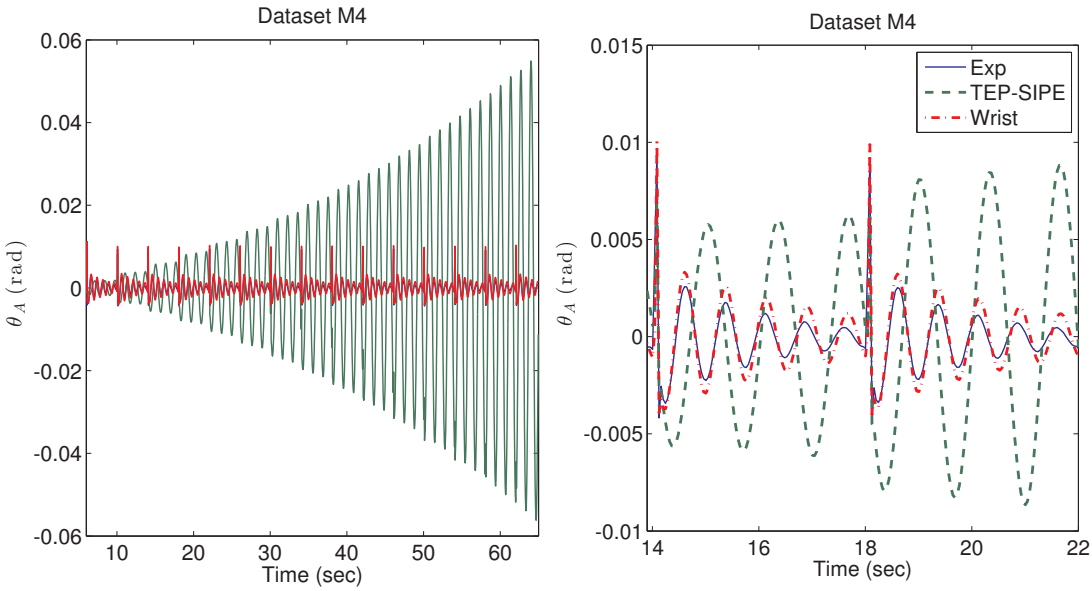

(a) Complete simulation **(b)** Short window of the simulation

Figure B-10: Minimum jerk perturbation with velocity amplitude 0.4 m/s

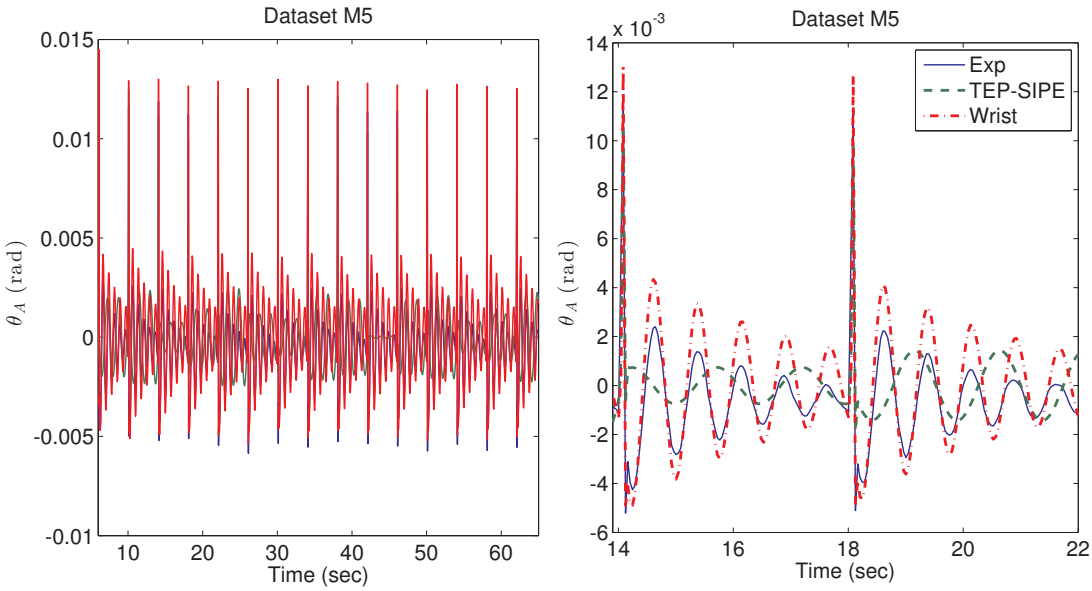

(a) Complete simulation **(b)** Short window of the simulation

Figure B-11: Minimum jerk perturbation with velocity amplitude 0.5 m/s

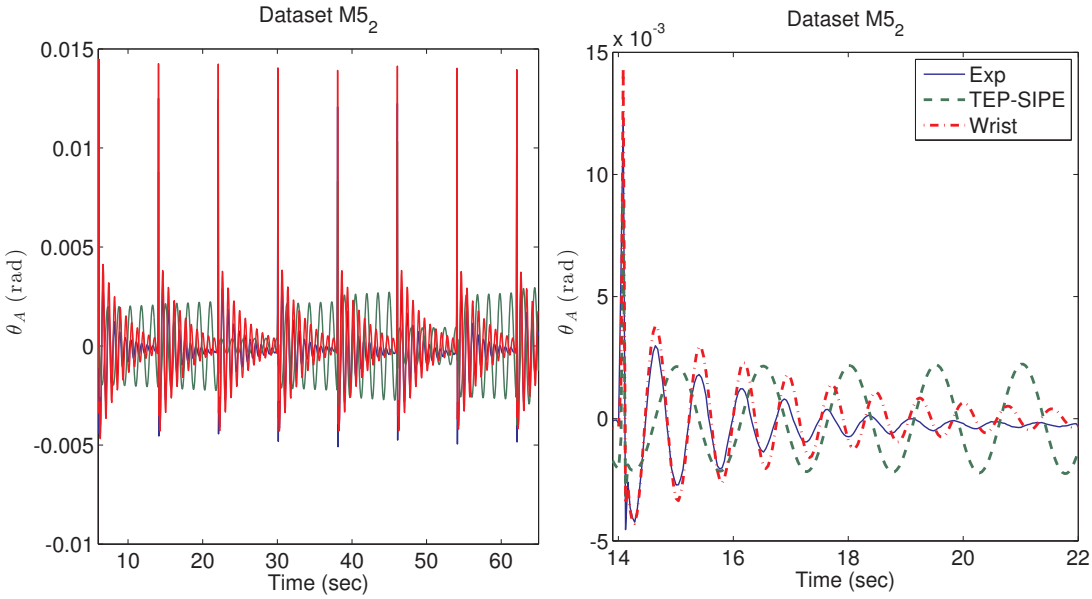

(a) Complete simulation

(b) Short window of the simulation

Figure B-12: Minimum jerk perturbation with velocity amplitude 0.5 m/s. Perturbations applied every 8 seconds.

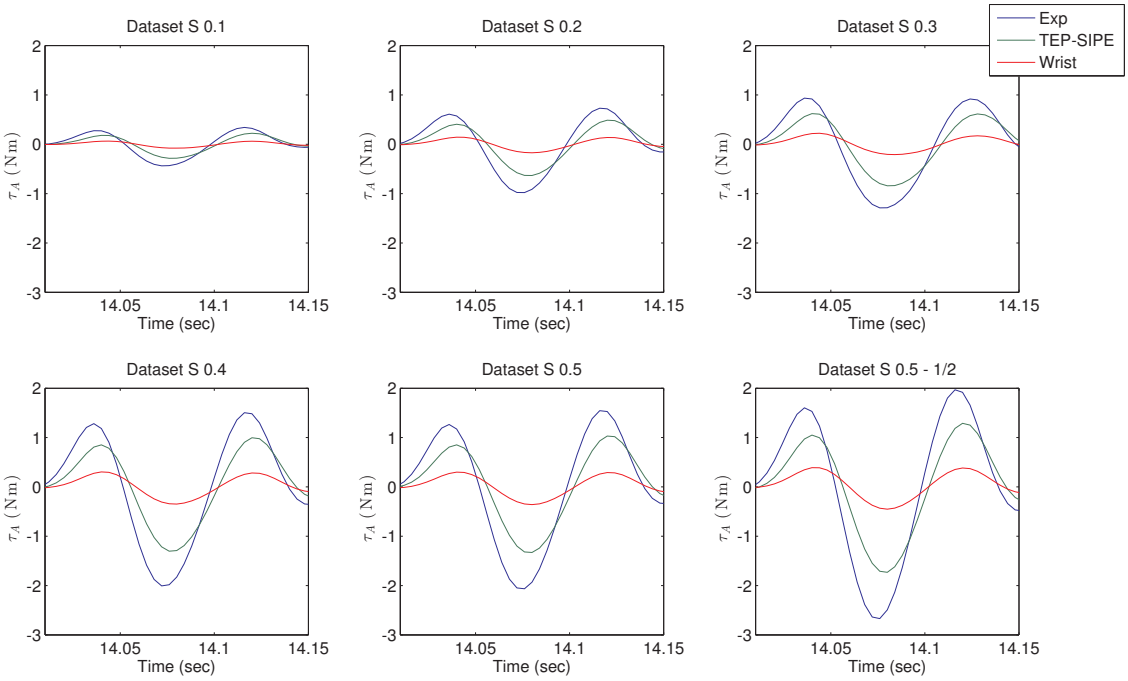

(a) Sinusoidal perturbation profiles

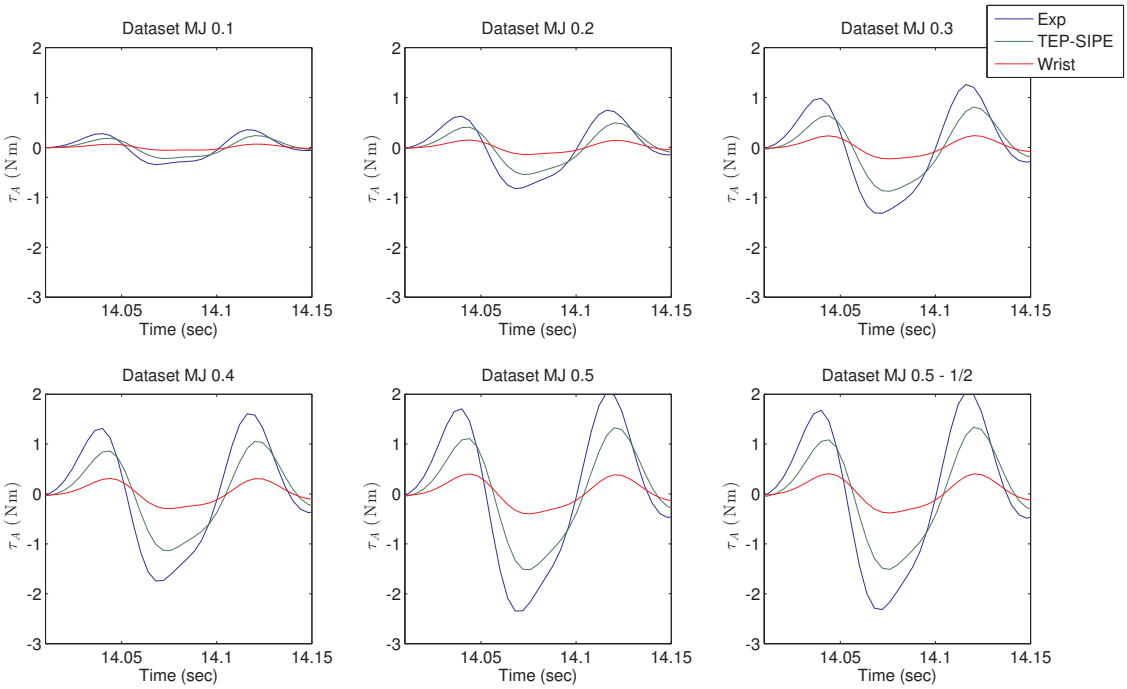

(b) Minimum jerk profiles

Figure B-13: Comparison of the measured τ_A and the simulated τ_{Asim}

Bibliography

[1] L. Ljung, "System identification: theory for the user," *Preniice Hall Inf and System Sciencess Series, New Jersey*, vol. 7632, 1987.

[2] M. Manto, N. Van Den Braber, G. Grimaldi, and P. Lammertse, "A new myohaptic instrument to assess wrist motion dynamically," *Sensors*, vol. 10, no. 4, pp. 3180–3194, 2010.

[3] E. J. Rouse, L. J. Hargrove, E. J. Perreault, and T. A. Kuiken, "Estimation of human ankle impedance during walking using the perturberator robot," in *Biomedical Robotics and Biomechatronics (BioRob), 2012 4th IEEE RAS & EMBS International Conference on*, pp. 373–378, IEEE, 2012.

[4] E. de Vlugt, A. C. Schouten, and F. C. van der Helm, "Quantification of intrinsic and reflexive properties during multijoint arm posture," *Journal of neuroscience methods*, vol. 155, no. 2, pp. 328–349, 2006.

[5] A. J. Stevenson, S. S. Geertsen, J. B. Andersen, T. Sinkjær, J. B. Nielsen, and N. Mrachacz-Kersting, "Interlimb communication to the knee flexors during walking in humans," *The Journal of physiology*, vol. 591, no. 19, pp. 4921–4935, 2013.

[6] S. Pfeifer, H. Vallery, M. Hardegger, R. Riener, and E. J. Perreault, "Model-based estimation of knee stiffness," *Biomedical Engineering, IEEE Transactions on*, vol. 59, no. 9, pp. 2604–2612, 2012.

[7] F. C. v. d. H. Herman Van der Kooij, Bart Koopman, "Human motion control." Reader for Delft University course wb2407 and Twente University course 115047, 2008.

[8] F. C. Van der Helm, A. C. Schouten, E. de Vlugt, and G. G. Brouwn, "Identification of intrinsic and reflexive components of human arm dynamics during postural control," *Journal of neuroscience methods*, vol. 119, no. 1, pp. 1–14, 2002.

[9] W. Mugge, D. A. Abbink, A. C. Schouten, J. P. Dewald, and F. C. van der Helm, "A rigorous model of reflex function indicates that position and force feedback are flexibly

tuned to position and force tasks," *Experimental brain research*, vol. 200, no. 3-4, pp. 325–340, 2010.

[10] R. E. Kearney, R. B. Stein, and L. Parameswaran, "Identification of intrinsic and reflex contributions to human ankle stiffness dynamics," *Biomedical Engineering, IEEE Transactions on*, vol. 44, no. 6, pp. 493–504, 1997.

[11] S. van Eesbeek, F. van der Helm, M. Verhaegen, and E. de Vlugt, "Lpv subspace identification of time-variant joint impedance," in *Neural Engineering (NER), 2013 6th International IEEE/EMBS Conference on*, pp. 343–346, IEEE, 2013.

[12] M. Mirbagheri, H. Barbeau, and R. Kearney, "Intrinsic and reflex contributions to human ankle stiffness: variation with activation level and position," *Experimental Brain Research*, vol. 135, no. 4, pp. 423–436, 2000.

[13] T. Sinkjaer, J. B. Andersen, and B. Larsen, "Soleus stretch reflex modulation during gait in humans," *Journal of Neurophysiology*, vol. 76, no. 2, pp. 1112–1120, 1996.

[14] E. J. Perreault, P. E. Crago, and R. F. Kirsch, "Estimation of intrinsic and reflex contributions to muscle dynamics: a modeling study," *Biomedical Engineering, IEEE Transactions on*, vol. 47, no. 11, pp. 1413–1421, 2000.

[15] L.-Q. Zhang, G. Nuber, J. Butler, M. Bowen, and W. Z. Rymer, "In vivo human knee joint dynamic properties as functions of muscle contraction and joint position," *Journal of biomechanics*, vol. 31, no. 1, pp. 71–76, 1997.

[16] R. E. Kearney and I. W. Hunter, "System identification of human joint dynamics.," *Critical reviews in biomedical engineering*, vol. 18, no. 1, pp. 55–87, 1989.

[17] J. Winters, L. Stark, and A.-H. Seif-Naraghi, "An analysis of the sources of musculoskeletal system impedance," *Journal of biomechanics*, vol. 21, pp. 1011–1025, 1988.

[18] D. Ludvig and E. Perreault, "System identification of physiological systems using short data segments," 2012.

[19] E. J. Perreault, P. E. Crago, and R. F. Kirsch, "Simultaneous estimation of intrinsic and reflex contributions to muscle dynamics: A modeling study," in *Engineering in Medicine and Biology Society, 1998. Proceedings of the 20th Annual International Conference of the IEEE*, vol. 5, pp. 2346–2349, IEEE, 1998.

[20] D. L. Guarin, K. Jalaleddini, and R. E. Kearney, "Identification of a parametric, discrete-time model of ankle stiffness," in *Engineering in Medicine and Biology Society (EMBC), 2013 35th Annual International Conference of the IEEE*, pp. 5065–5070, IEEE, 2013.

[21] T. Sinkjaer, E. Toft, S. Andreassen, and B. C. Hornemann, "Muscle stiffness in human ankle dorsiflexors: intrinsic and reflex components," *Journal of Neurophysiology*, vol. 60, no. 3, pp. 1110–1121, 1988.

[22] R. Kearney, H. Giesbrecht, M. Baker, D. Ludvig, and R. Wagner, "Identification of time-varying intrinsic and reflex joint stiffness," in *Engineering in Medicine and Biology Society, 2006. EMBS'06. 28th Annual International Conference of the IEEE*, pp. 288–291, IEEE, 2006.

[23] I. Ulrich, "Combining transient and continuous identification techniques to investigate human reflexes," Master's thesis, TU Delft, 2012.

[24] A. C. Schouten, E. de Vlugt, and F. C. van der Helm, "Design of perturbation signals for the estimation of proprioceptive reflexes," *Biomedical Engineering, IEEE Transactions on*, vol. 55, no. 5, pp. 1612–1619, 2008.

[25] E. J. Perreault, R. F. Kirsch, and P. E. Crago, "Multijoint dynamics and postural stability of the human arm," *Experimental brain research*, vol. 157, no. 4, pp. 507–517, 2004.

[26] T. A. Boonstra, A. C. Schouten, and H. van der Kooij, "Identification of the contribution of the ankle and hip joints to multi-segmental balance control," *Journal of neuroengineering and rehabilitation*, vol. 10, no. 1, p. 23, 2013.

[27] J. H. Pasma, T. A. Boonstra, S. F. Campfens, A. C. Schouten, and H. Van der Kooij, "Sensory reweighting of proprioceptive information of the left and right leg during human balance control," *Journal of neurophysiology*, vol. 108, no. 4, pp. 1138–1148, 2012.

[28] E. J. Perreault, R. F. Kirsch, and A. M. Acosta, "Multiple-input, multiple-output system identification for characterization of limb stiffness dynamics," *Biological cybernetics*, vol. 80, no. 5, pp. 327–337, 1999.

[29] R. Toth, *Modeling and identification of linear parameter-varying systems*, vol. 403. Springer, 2010.

[30] H. Lee, H. I. Krebs, and N. Hogan, "A novel characterization method to study multivariable joint mechanical impedance," in *Biomedical Robotics and Biomechatronics (BioRob), 2012 4th IEEE RAS & EMBS International Conference on*, pp. 1524–1529, IEEE, 2012.

[31] H. Kristinsdottir, "Estimating ankle joint impedance in the stance phase of gait using an instrumented treadmill," Master's thesis, TU Delft, 2013.

[32] A. C. Schouten, E. de Vlugt, J. Van Hilten, and F. C. van der Helm, "Design of a torque-controlled manipulator to analyse the admittance of the wrist joint," *Journal of neuroscience methods*, vol. 154, no. 1, pp. 134–141, 2006.

[33] D. T. Westwick and R. E. Kearney, *Identification of Nonlinear Physiological Systems*. Wiley Online Library, 2003.

[34] E. J. Rouse, L. J. Hargrove, E. J. Perreault, M. A. Peshkin, and T. A. Kuiken, "Development of a mechatronic platform and validation of methods for estimating ankle stiffness during the stance phase of walking," *Journal of biomechanical engineering*, vol. 135, no. 8, p. 081009, 2013.

[35] B. Koopman, E. Van Asseldonk, and H. Van Der Kooij, "In vivo measurement of human knee and hip dynamics using mimo system identification," in *Engineering in Medicine and Biology Society (EMBC), 2010 Annual International Conference of the IEEE*, pp. 3426–3429, IEEE, 2010.

List of Acronyms

UMND	Upper Motor Neuron Disease
SIPE	System Identification and Parameter Estimation
DoF	Degree-of-Freedom
SNR	Signal-to-Noise Ratio
TEP	Transient Endpoint Perturbations
CoM	Center of Mass